# MODELING FX OPTIONS IN PRESENCE OF STOCHASTIC VOLATILITY WITH OVERNIGHT-INDEXED-SWAP-DISCOUNTING

A THESIS SUBMITTED TO
THE GRADUATE SCHOOL OF APPLIED MATHEMATICS
OF
MIDDLE EAST TECHNICAL UNIVERSITY

BY

SELİN TEKTEN

IN PARTIAL FULFILLMENT OF THE REQUIREMENTS
FOR
THE DEGREE OF MASTER OF SCIENCE
IN
FINANCIAL MATHEMATICS

DECEMBER 2019

Approval of the thesis:

**MODELING FX OPTIONS IN PRESENCE OF STOCHASTIC VOLATILITY WITH OVERNIGHT-INDEXED-SWAP-DISCOUNTING**

submitted by **SELİN TEKTEN** in partial fulfillment of the requirements for the degree of **Master of Science in Department of Financial Mathematics, Middle East Technical University** by,

Prof. Dr. Ömür Uğur
Director, Graduate School of **Applied Mathematics** _____

Prof. Dr. A. Sevtap Selçuk-Kestel
Head of Department, **Financial Mathematics** _____

Prof. Dr. Ömür Uğur
Supervisor, **Scientific Computing** _____

**Examining Committee Members:**

Prof. Dr. A. Sevtap Selçuk-Kestel
Financial Mathematics, IAM, METU _____

Prof. Dr. Ömür Uğur
Scientific Computing, IAM, METU _____

Assoc. Prof. Dr. Ümit Aksoy
Department of Mathematics, Atılım University _____

**Date:** _____

**I hereby declare that all information in this document has been obtained and presented in accordance with academic rules and ethical conduct. I also declare that, as required by these rules and conduct, I have fully cited and referenced all material and results that are not original to this work.**

**Name, Last name : SELİN TEKTEN**

**Signature :** _____

# ABSTRACT

MODELING FX OPTIONS IN PRESENCE OF STOCHASTIC VOLATILITY
WITH OVERNIGHT-INDEXED-SWAP-DISCOUNTING

Tekten, Selin
M.Sc. , Department of Financial Mathematics
Supervisor: Prof. Dr. Ömür Uğur

December 2019, 76 Pages

This study investigates the time contingent behavior of risk factor USDTRY. Option pricing models Black-Scholes and Heston has been utilized to estimate the behavior. The adjusted Black-Sholes model is the current market practice to model USDTRY risk factor. Market practitioners do not prefer to use constant volatility in the Black-Scholes Model, which violates the model assumption. They instead interpolate the volatility surface from market data of implied volatilities and use them in Black-Scholes Model. However, Heston model admits varying volatilities. The Heston Model adds a dimension to the Black-Scholes model by letting the volatility to be a stochastic process. In this thesis, we have used interpolated volatility surface as a benchmark for testing the results estimated by the Heston Model. Furthermore, while estimating option prices, Overnight-Indexed-Swap (OIS) discounting framework has been governed to achieve risk-free rates. The test results have indicated that Heston stochastic volatility model

with OIS discounting offers arbitrage-free pricing with similar computation efficiency to the benchmark.

**Keywords**: Currency Options, USDTRY, Heston Model, Overnight-Indexed-Swap Discounting, Volatility Surface

# ÖZ

STOKASTİK VOLATİLİTE ALTINDA, GECELIK VADEYE ENDEKSLI SWAP İSKONTO YÖNTEMİ İLE KUR OPSİYONLARININ MODELLENMESİ

Tekten, Selin
M.Sc. , Department of Financial Mathematics
Supervisor: Prof. Dr. Ömür Uğur

Aralık 2019, 76 Sayfa

Bu çalışma, risk faktörü USDTRY'nin zamana bağlı davranışını incelemektedir. Opsiyon fiyatlama modelleri Black-Sholes ve Heston bu davranışı tahmin etmek için kullanılmıştır. Düzeltilmiş Black-Sholes modeli, USDTRY riskfaktörü modellemesinde güncel piyasa pratiğidir. Piyasa uygulayıcıları, Black-Scholes modelinde sabit volatilite kullanmazlar, ki bu model varsayımına aykırıdır. Bunun yerine, volatilite yüzeyini, piyasada gözlemlenen ima edilen volatilitelerden enterpole ederek oluşturur ve Black-Scholes modelinde kullanırlar. Heston modelinde ise, değişken volatile varsayım dahilindedir. Heston modeli, volatiliteyi stokastik bir süreç olarak varsayarak, Black-Scholes modelinin üzerine bir boyut daha ekler. Bu çalışmada, Heston modelinin tahmin

sonuçlarını test etmek için enterpole edilmiş volatilite yüzeyini referans olarak kullandık. Ayrıca, opsiyon fiyatlarının tahmininde kullanılacak risksiz-faiz-oranlarını, gecelik vadeye endeksli swap iskonto yöntemi ile inşa ettik. Test sonuçları, gecelik vadeye endeksli swap iskonto yöntemi kullanılan Heston stokastik volatilite modelinin, seçilen referansa yakın hesaplama verimliliği sağlarken, arbitrajsız fiyatlama imkanı sunduğunu göstermektedir.

**Anahtar Sözcükler**: Kur Opsiyonları, USDTRY, Heston Model, Gecelik-Vadeye-Endeksli-Swap İskonto Yöntemi, Volatilite Yüzeyi

*To My Beloved Family and My Beloved Cousin Aslı*

## ACKNOWLEDGMENTS

First of all, I would like to express my gratitude to my thesis advisor Professor Dr. Ömür Uğur, for kindness, patient guidance, enthusiastic encouragement, and valuable advice he provided in the development and preparation of this thesis. His willful giving of their time and to share their experiences has brightened my path.

I would also like to thank my family, friends, and colleagues for their patience, love, and encouragement and the kindness and help of members of the Institute of Applied Mathematics.

## TABLE OF CONTENTS

## LIST OF TABLES

## LIST OF FIGURES

## LIST OF ABBREVIATIONS

| | |
|---|---|
| ACT | Actual |
| ATM | At-the-money |
| BF | Butterfly Spread |
| FX | Foreign Exchange |
| IRS | Interest Rate Swap |
| LIBOR | London Inter-Bank Offered Rate |
| OIS | Overnight Indexed Swap |
| ON | Overnight |
| OTC | Over the counter |
| RR | Risk-reversal |
| TN | Tomorrow-next |
| TRY | Turkish Lira |
| USD | United States Dollar |

# CHAPTER 1

## OVERVIEW

Interest rate differential benefits on foreign exchange markets in Turkey, entail high trade volume and variety of financial derivatives. The exposure to foreign exchange brings protection needs and permits complex hedging activities. Investors develop hedging strategies against their exchange rate exposure. Their transactions generate a liquid foreign exchange market.

The fact that the average daily volume of the market in Turkey is estimated to be around 22 billion US Dollars [2] indicates the size of the market. About 90% of this turnover consists of spot deals and foreign exchange swaps. Central-banks, commercial companies, and funds form a significant part of the market. Because actors of the foreign exchange market make large transactions, and also, they perform small deals, the market is split into levels of access that we cannot see in the stock exchange markets. As an inevitable outcome of this large volume of transactions, the majority of the trades are performed in the over-the-counter (OTC) market. Biggest commercial banks, security traders perform their deals in the inter-bank market. Since bigger trading size occurred at the top of this degree of access, ask-bid spreads of the currencies are narrower relative

to the lower degree of access. Ask-bid spread of currencies widens as go to the lower degree.

In this study have focused on the FX-OTC market, since it is great in demand and offers liquid option quotations. The foreign exchange market has own specific conventions. Currency options' deals do not consist of single options with a particular strike, unlike stocks exchange markets apply. Quotes on currency options address the portfolio of options based on specific deltas.

In section 2.1, we have argued about resolve foreign exchange market conventions. Translation of the quotes into a standard format that financial models consume occurs in two steps; the first step is reversing the portfolio to single options; the next step is converting delta-implied volatility pairs into strikes. After relevant mapping, vanilla options data have been properly arranged to be involved in the calibration of pricing models, Heston, and Black Scholes. We have benefited the study [9], for the conversion of the option quotations and examining terms and conditions of USDTRY options. We have extended the scope of the study of Eratman [9], by using options with time-to-maturity of 1-month, 2-month, 3-month, 6-month, 9-month, and 12-month instead of using only 1-month option data. We have adopted the approach of [18], by setting aside a part of the data (2-month and 9-month) to use them in out-sample tests later on.

During the calibration, due to the assumptions Heston and Black-Scholes models, we have also required risk-free rate data. The risk-free rate considered in the

valuation of options should be the rate at which banks supply the cash and must create a dynamic hedging portfolio that will replicate the final payoff at expiry.

In section 2.2, we have constructed risk-free, zero-coupon discount curves for USD and TRY. In the formation of USD risk-free, zero-coupon discount curve, we have benefited from quotations on Overnight-Indexed-Swaps. This framework has been widely accepted in the literature, see [12]. We have designed a much-complicated set up for TRY risk-free, zero-coupon discount curve. Since we have not got any liquidly traded derivatives on the TRY floating rate index like LIBOR, we have used information on foreign exchange instruments by applying interest rate parity. Thanks to findings of Kazdal and Küçüksaraç, see [14], we have taken FX swap points to construct the curve. However, to be able to build the TRY yield curve, we have also needed to construct a zero-coupon curve for 3m USD LIBOR to achieve fixed values for 3m USD LIBOR. This approach is known to be used by some private banks. However, to our knowledge, this study is the first one that considers the OIS yield curve construction for the TRY.

In section 4.1, we analyzed historical data of USDTRY observed between 11 March 2013 and 20 August 2018.

We have dedicated chapter 3, to describe the dynamics of the models.

In section 4.2, we have calibrated and tested the results. We have used both unit weights and liquidity-weights on the calibration procedure. We have extended the scope of We have considered in-sample and out-sample measure performances. Namely, we have compared the estimates and real data, and, afterward, we have estimated for different prices whose market-prices have not been involved during the calibration.

Furthermore, we have studied model-generated implied volatilities if they can stay in the bid-ask range. Otherwise, they may generate instantaneous arbitrage opportunity in market conditions. To our knowledge, this bid-ask range control has not mentioned in the literature. We have presented details of the tests in which the Heston model has comparable results with the benchmark.

# CHAPTER 2

## PRELIMINARIES

Unlike stock exchange markets, foreign exchange options market data represented based on options delta, instead of option prices by a strike. Moreover, the quotations expressed for a portfolio of options contracts rather than an individual option.

Implied volatilities of foreign exchange options are represented based on maturities and deltas. Delta is one of the essential exposures to an options trader. It is the sensitivity of the price of the option to a change in the underlying asset.

Since in the models we use in this study generate option prices depending on strike prices, we must map delta-based volatility to strike-based volatility data. However, delta has various formulations in the foreign exchange market. We present the details of the terms and conditions for the USDTRY currency pair in the following section.

## 2.1 Foreign Exchange Market Conventions

### 2.1.1 FX Forward Value

At the beginning, by rule of no-arbitrage, value of an outright forward contract is equals to zero. Then, as foreign exchange rates and/or interest rates change, the forward contract has value of different from zero, yet is the following [19],

$$\upsilon_f(\tau) \;=\; e^{-r_d\tau}(f(t,T)-K) = S_t e^{-r_f\tau} - Ke^{-r_d\tau}.$$

### 2.1.2 Terms and Conditions

Since the credit crunch of 2008 and the associated low levels of liquidity in short-term interest rate products, it became unfeasible for banks to agree on spot deltas (which include discount factors) [6].

When the underlying currency pair includes one of the emerging market currencies or maturity of the option is longer than one year, the market practice is to use forward delta. Forward delta convention is employed exclusively in the construction of the FX smile, which does not involve any discounting. The reason for this condition is that the discount factor shows itself as longer maturity is considered or high-interest rates are considered in the emerging markets. These options are utilized to hedge with the forward-contracts. In the case of the USDTRY over-the-counter options market, the delta convention corresponds to forward-delta, and the ATM type corresponds to forward-delta-neutral case, for details see [9].

#### 2.1.2.1 Forward Delta

Forward delta is formulated with the derivative of Black-Scholes value υ for the option with respect to forward price of the underlying asset $\upsilon_f(\tau)$,

$$\Delta_{\mathrm{f}}(\mathrm{K},\sigma,\phi) \;=\; \frac{\partial \upsilon}{\partial \upsilon_f} = \frac{\partial \upsilon}{\partial \mathrm{S}}\frac{\partial \mathrm{S}}{\partial \upsilon_f} = \frac{\partial \upsilon}{\partial \mathrm{S}}\left(\frac{\partial \upsilon_f}{\partial \mathrm{S}}\right)^{-1} \tag{2.1}$$

$$\Delta_f(K,\sigma,\phi) \;=\; \phi \mathrm{N}(\phi d_+), \tag{2.2}$$

where $\phi$ is a binary function of option class, which takes 1 for call options and, $-1$ for put options, $N(x)$ is the cumulative distribution function of standard normal distribution, $d_+ = \frac{\ln\frac{f}{K}+\frac{1}{2}\sigma^2\tau}{\sigma\sqrt{\tau}}$, and, $f$ denotes forward rate, $K$ is the option strike price, and, $\sigma$ denotes implied volatility (by Black-Scholes model). This yields a Put-Call delta parity as stated in a previous study [9],

$$\Delta_f(\mathrm{K},\sigma,1) - \Delta_f(\mathrm{K},\sigma,-1) \;=\; 1. \tag{2.2}$$

In foreign exchange market, one must enter to a multiple of $\Delta_f \times N$ number of forward contracts in favor of hedging a short vanilla position. Forward delta type is mostly governed convention in majority of the currency pairs, since the absolutes of delta of a call and put totals to 1; namely, $10\Delta P$ and $90\Delta P$ have the same volatilities. In addition, deciphering of the strike volatility pairs from delta volatility is required for the calibration phase. So, the strike price formula for forward delta type is given by,

$$K \;=\; f\exp\left\{-\phi N^{-1}\left(\phi\Delta_f\right)\sigma\sqrt{\tau}+\frac{1}{2}\sigma^2\tau\right\}, \tag{2.3}$$

where $\phi$ is a binary function of option class, which takes 1 for call options and, $-1$ for put options, $N(x)$ denotes the cumulative distribution function of standard normal

distribution, $f$ denotes forward rate, $K$ is the option strike price, $\Delta_f$ denotes forward-delta and, $\sigma$ denotes implied volatility (by Black-Scholes model).

### 2.1.3 Foreign Exchange Vanilla Quotes

Foreign exchange market structures deep volatility smile shape. Current market practice is to trade volatility smile factors rather than individual vanilla options. A combination of vanilla options at different deltas is used to catch the volatility smile dynamics. Examples of liquidly traded a portfolio of options are at-the-money straddles, risk reversals, and butterfly spreads, whose delta are typically 0.10 or 0.25.

#### 2.1.3.1 At-the-Money Options

Traders denote prices of options on currencies and precious metals as Black-Scholes implied volatilities. As assumed in the study of Eratman in [9], the exercise-price of an USDTRY at-the-money option corresponds to the current forward rate of time to maturity equals to the option tenor, rather than the spot-exchange-rate. This option convention is referred to as at-the-money forward, hereafter denoted by ATM as in [15]; and

$$\sigma_{ATM} = \sigma(t, \Delta, \tau | K_{\Delta} = f), \qquad (2.4)$$

where $f$ is the forward rate, and $\Delta$ is the delta value (that equals to the forward rate) as the strike.

#### 2.1.3.2 Risk Reversal

A risk reversal is a portfolio of options which is built as difference (being long and short) of two options: a call option with a high exercise price and a put option with a low

exercise price both having the same time-to-maturity. Mostly, these two exercise prices imply different implied volatilities, and market quotation refers to the difference of the implied volatilities of those options. This quotation is named as the "risk reversal of the implied volatility smile" or shortly "the smile risk reversal". The direction of that difference of implied volatilities is specified based on the market practice of order. Market practitioners mostly adopt the direction that will yield non-negative portfolio value. In this case, every market player admits the side of implied volatilities is eminent for the market taken into consideration. In the lack of certainty of the direction of risk reversal quotes, to emphasize the direction. They used the phrase "bid for" for the options with higher volatility. The direction is often characterized through the out-of-the-money option with option type (call option or put option) of a currency in the currency pair (i.e., currency other than USD if USD is in the currency pair). In USDTRY options, higher implied volatilities are observed in options with a high exercise price. Thus, one would declare "bid for the high side" or "bid for TRY puts". We can compute the risk reversal of the implied volatility smile by taking a long position in the high-exercise-price implied volatility and taking a short position in the low- exercise-price implied volatility.

The risk reversal related to skewness in the smile [7]. For instance, if we let $\sigma_{25\Delta RR}$ stand for the 25-delta-risk reversal quote for USDTRY. Then the 25-delta-call and 25-delta-put options' implied volatility difference is amount to the risk reversal quote,

$$\sigma_{25\Delta RR} = \sigma_{25\Delta call} - \sigma_{25\Delta put} . \quad (2.5)$$

#### 2.1.3.3 Butterfly Spread

A strangle is the mean of long out of-the-money put and call option. A strangle margin is referred to as the difference between the strangle volatility and the ATM volatility. The butterfly quote implies to this difference and, describes how convex the smile is. Again, if we let $\sigma_{25\Delta BF}$ express the 25-delta-butterfly quote. So,

$$\sigma_{25\Delta BF} = \frac{\sigma_{25\Delta call} + \sigma_{25\Delta put}}{2} - \sigma_{ATM} . \quad (2.6)$$

Figure 2.1 demonstrates risk reversal and skew relation and butterfly and convexity relation. ATM quotations give a parallel shift of volatility smile, Risk reversal spread lets the slope of the smile more prominent, and butterfly spread effects the curviness of smile.

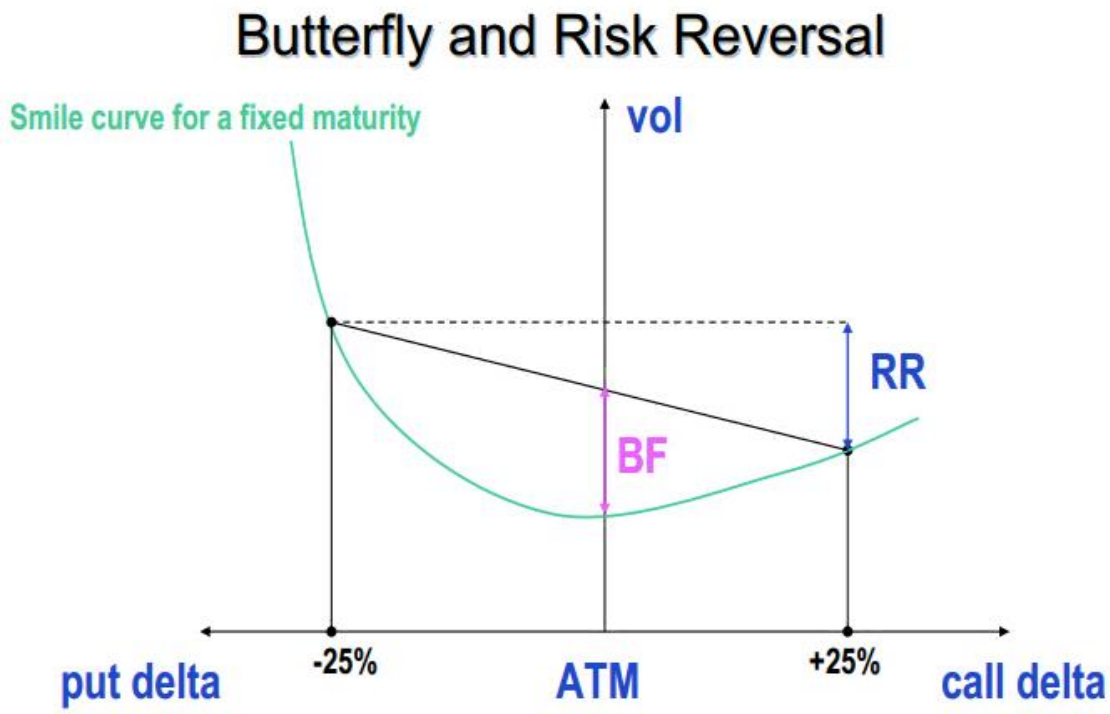


Figure 2.1 Butterfly and Risk Reversal, [23].Graphic representation of the butterfly and risk reversal. It could be observed that the risk reversal spread widens as skew increases. Moreover, butterfly appreciates, as degree of curvature of the smile increases (Namely the bigger the second derivative).

## 2.2 Yield Curve Construction

If we let option valuation, to be based on forming a dynamic hedging portfolio that will replicate the final payoff at expiry, we should find at which rate banks must supply the cash to create such portfolio. OTC dealers borrow and lend at a rate based on LIBOR, which is the funding rate for large commercial banks. Therefore, We have not used the Government bond yield curve in this study.

There has lately been a move from LIBOR-indexed swaps to OIS based swaps along with the OIS-LIBOR spread has been widened. The spread expanded to be

apparent in the time of the financial crisis in 2008. OIS discounting has become the market practice in the valuation of collateralized instruments, and clearinghouses require it.

Similar to an interest rate swap, OIS contracts comprise the exchange of only the interest cash flows; the principal amount equals to notional. Namely, counterparties deal to exchange, on the designated notional amount, the difference between interest accrued at the fixed rate, which agreed upon at inception and interest accrued by daily compounding (generally, the geometric average is used) of the floating overnight index rate.

Since the OIS market being very liquid for dominant currencies, besides liquid quotation involves a wide range of maturities, those OIS quotes can effectively calibrate a discount curve by benefiting standard approaches and, can be employed to discount collateralized derivative instruments.

We have used OTC market data of options in t calibration of models Heston and Black-Scholes. Besides, most OTC market transactions are subjected to a collateral agreement.

As stated by Hull et. Al in [12], overnight rate yield curves implied by OIS should be used as a risk-free rate even though the portfolio is not collateralized. Hence, we have used the OIS based yield curve as a proxy of the risk-free rate in this study.

In the scope of this study, we build yield curves up to 1-year tenor. We aim to estimate the discounting curve for currency TRY and currency USD.

We have fitted the discounting curve for currency TRY, to foreign exchange swaps and cross-currency swaps as opposed to OIS discounting framework. However, we have discounted USD currency-denominated cash flows of those foreign exchange instruments with USD Discount Curve (fitted to OIS mid-market quotes). Hence, We have addressed the OIS discounting in the TRY Discount Curve. However, we require a forward curve for 3m USD LIBOR to find the floating rates of the future cash flows of the above-mentioned cross-currency swap. Furthermore, again, the forward curve of 3m USD LIBOR is constructed by referring discount factors from USD discounting curve (OIS curve).

### 2.2.1 USD Discount Curve

As stated in the previous section, we have constructed the discount curve for USD on information from overnight indexed swap contracts written on the effective-fed-funds-overnight-rate.

OIS refers to an interest rate swap that exchanges a fixed-rate coupon for a floating rate coupon, which is a daily compounded overnight rate, where the dates of the two coupon payments typically coincide. Hence, the floating payment for a period $[t, T]$ will be

$$\prod_{i=0}^{K-1}\left(1 + \alpha(t_i, t_{i+1})\boldsymbol{FF}(t_i, t_{i+1})\right) - 1, \tag{2.7}$$

where

$K$: number of all the business days in the time interval $[t, T]$

$\{t_i\}_{i=0}^{K}$: all the business days in the accrual period $[t, T]$ with $t_0$ = t and $t_k = T$

$\boldsymbol{FF}(t_i, t_{i+1})$: represents the overnight interest rate for the period $(t_i, t_{i+1})$

$\alpha(t_i, t_{i+1})$: the year fraction between $t_i$ and $t_{i+1}$ according to a market convention.

Now we consider the calculation of the net present value of a payer OIS contract. At time $t$, if we us enter into a payer OIS with $N$ coupons, payments dates at $T_1 < T_2 < \cdots < T_N$ and $T_0 - t$ days of spot lag. Assume that we pay a fixed rate $k$ and receive a floating rate (daily compounded overnight rate). Then, by (2.7) the $i$th floating leg rate $\boldsymbol{FFComp}(T_{i-1}, T_i)$ is given by

$$\boldsymbol{FFComp}(T_{i-1}, T_i) = \frac{1}{\sum_{j=0}^{K_{i-1}} \alpha(t_j, t_{j+1})} \left( \prod_{j=0}^{K-1} \left(1 + \alpha(t_j, t_{j+1}) \boldsymbol{FF}(t_j, t_{j+1})\right) - 1 \right). \quad (2.8)$$

Here we recall that $\sum_{j=0}^{K_{i-1}} \alpha(t_j, t_{j+1}) = \alpha(T_j, T_{j+1})$. Thus, by setting $\delta$ such that $e^{\delta t} = 1 + it$, then it yields

$$\begin{aligned} \prod_{j=0}^{K_i-1} \left(1 + \alpha(t_j, t_{j+1}) \boldsymbol{FF}(t_j, t_{j+1})\right) - 1 &= e^{\ln\left(\prod_{j=0}^{K_i-1}\left(1+\alpha(t_j,t_{j+1})\boldsymbol{FF}(t_j,t_{j+1})\right)\right)} - 1 \\ &= e^{\sum_{j=0}^{K_i-1} \ln\left(1+\alpha(t_j,t_{j+1})\boldsymbol{FF}(t_j,t_{j+1})\right)} - 1 \\ &= e^{\sum_{j=0}^{K_i-1} \alpha(t_j,t_{j+1})\delta(t_j,t_{j+1})} - 1. \quad (2.9) \end{aligned}$$

In the equation (2.9) the term $\sum_{j=0}^{K_i-1} \alpha(t_j, t_{j+1}) \delta(t_j, t_{j+1})$ is equal to the Riemann sum of function $\delta$ with partition $\mathcal{P} = \{[t_0, t_1], [t_1, t_2], \ldots [t_{K_i-1}, t_{K_i}]\}$. So,

$$\sum_{j=0}^{K_i-1} \alpha(t_j, t_{j+1}) \delta(t_j, t_{j+1}) \approx \int_{T_i-1}^{T_i} \delta(s) ds.$$

And, the no arbitrage principle, price of an instrument must be equal to its expected cash flows. Then, the present value of a payer OIS contract (pays fixed rate, receives floating rate) becomes:

$$
\begin{aligned}
PV(t) &= \sum_{\mathrm{i}=1}^{\mathrm{N}} \tau(\mathrm{T_{i-1}}, \mathrm{T_i}) \mathbb{E}_{\mathrm{t}} \left[ \mathrm{e}^{-\int_{\mathrm{t}}^{\mathrm{T_i}} \delta(\mathrm{s}) \mathrm{ds}} \mathbf{FFComp}(\mathrm{T_{i-1}}, \mathrm{T_i}) - \mathrm{k} \right] \\
&= \sum_{i=1}^{\mathrm{N}} \tau(T_{\mathrm{i-1}}, T_{\mathrm{i}}) \mathbb{E}_{\mathrm{t}} \left[ e^{-\int_t^{T_i} \delta(s) ds} \left( \frac{1}{\sum_j \alpha(t_j, t_{j+1})} \left( \prod_{j=0}^{K_i - 1} \left( 1 \right. \right. \right. \right. \\
&\qquad \left. \left. \left. \left. + \alpha(t_j, t_{j+1}) \boldsymbol{FF}(t_j, t_{j+1}) \right) - 1 \right) - k \right) \right] \\
&= \sum_{i=1}^{\mathrm{N}} \tau(T_{\mathrm{i-1}}, T_{\mathrm{i}}) \mathbb{E}_{\mathrm{t}} \left[ e^{-\int_t^{T_i} \delta(s) ds} \left( \frac{1}{\tau(T_{\mathrm{i-1}}, T_{\mathrm{i}})} \left( e^{\int_{T_{i-1}}^{T_i} \delta(s) ds} - 1 \right) - k \right) \right] \\
&= \sum_{i=1}^{\mathrm{N}} \mathbb{E}_{\mathrm{t}} \left[ e^{-\int_t^{T_i} \delta(s) ds} \left( e^{\int_{T_{i-1}}^{T_i} \delta(s) ds} - 1 \right) \right] - k \sum_{i=1}^{\mathrm{N}} \tau(T_{\mathrm{i-1}}, T_{\mathrm{i}}) \mathbb{E}_{\mathrm{t}} \left[ e^{-\int_t^{T_i} \delta(s) ds} \right] \\
&= \sum_{i=1}^{\mathrm{N}} \mathbb{E}_{\mathrm{t}} \left[ e^{-\int_t^{T_{i-1}} \delta(s) ds} - e^{\int_t^{T_i} \delta(s) ds} \right] - k \sum_{i=1}^{\mathrm{N}} \tau(T_{\mathrm{i-1}}, T_{\mathrm{i}}) \mathbb{E}_{\mathrm{t}} \left[ e^{-\int_t^{T_i} \delta(s) ds} \right] \\
&= \sum_{i=1}^{\mathrm{N}} P(t, T_{i-1}) - P(t, T_i) - k \sum_{i=1}^{\mathrm{N}} \tau(T_{\mathrm{i-1}}, T_{\mathrm{i}}) P(t, T_i) \\
&= P(t, T_0) - P(t, T_N) - k \sum_{i=1}^{N} \tau(T_{i-1}, T_i) P(t, T_i). \qquad (2.10)
\end{aligned}
$$

Accordingly, if we suppose that the fixed rate $k$ is a mid-market quote, then, by no-arbitrage arguments what we get is that the present value of the OIS is equal to zero. Therefore, when (2.10) is equal to zero it yields,

$$P(t,T_N) = \frac{P(t,T_0) - k\sum_{i=1}^{N-1}\tau(T_{i-1},T_i)P(t,T_i)}{1+k\tau(T_{N-1},T_N)}. \quad (2.11)$$

This equation represents the bootstrapping equation associated to the $N$-coupons OIS contract. Here we recall that we have $N+1$ variables $P(t,T_0), P(t,T_1), \dots, P(t,T_N)$ and only one equation. Hence, one needs to obtain more OIS contracts to obtain more bootstrapping equations and a method to figure out this system of equations.

In the USD OIS market, cashflows of the swaps with maturities no longer than a year normally consist of one payment at maturity, while swaps with a maturity over a year normally consist of yearly payments. In the scope of this study, contracts of maturity up to one year is used to construct the yield curve. So following the trimmed version of (2.11) will be sufficient, in our study, Namely, we will use

$$P(t,T_X) = \frac{P(t,T_0)}{1+k_X\tau(T_0,T_X)}, \quad (2.12)$$

where

$$\begin{aligned} P(t,T_0) &= P(t,t+2) = P(t,t+1)P(t+1,t+2) \\ &= \frac{1}{1+\tau(t,t+1)ON}\cdot\frac{1}{1+\tau(t+1,t+2)TN}. \end{aligned} \quad (2.13)$$

Given that spot lag for USD OIS contracts is two business days and, *ON* represents overnight effective fed funds rate, *TN* represents effective fed funds rate of term for tomorrow to the next day period. In Table 2.1 we present the market data used in the estimation of the USD discount curve. ACT/360 in Table 2.1 is a day count convention by formula,

$$Day\ Count\ Factor_{ACT/360}(t_1, t_2) = \frac{Number\ of\ Calendar\ Days(t_1, t_2)}{360}.$$

Table 2.1: USD Discount Curve Bloomberg Data. Bloomberg market data terms and conditions table referred in calibration of USD discount curve. Quotes are End of Day prices from 20/08/2018.

| Tenor | Bloomberg Ticker | Type | Start day | End day | Rate | Floating Leg Period | Floating Leg Business Day Rule | Floating Leg Business Day Count | Fixed Leg Period | Fixed Leg Business Day Rule | Fixed Leg Business Day Count |
|---|---|---|---|---|---|---|---|---|---|---|---|
| ON | FEDL01 | Cash | 0d | 1d | 1.441 | - | Following | ACT/360 | - | - | - |
| TN | FEDL01 | Cash | 1d | 1d | 1.441 | - | Following | ACT/360 | - | - | - |
| 1W | USSO1Z | OIS | 2d | 1w | 1.6814 | 1w | Mod. Fol. | ACT/360 | 1y | Mod. Fol. | ACT/360 |
| 2W | USSO2Z | OIS | 2d | 2w | 1.6707 | 2w | Mod. Fol. | ACT/360 | 1y | Mod. Fol. | ACT/360 |
| 3W | USSO3Z | OIS | 2d | 3w | 1.673 | 3w | Mod. Fol. | ACT/360 | 1y | Mod. Fol. | ACT/360 |
| 1M | USSOA | OIS | 2d | 1m | 1.673 | 1m | Mod. Fol. | ACT/360 | 1y | Mod. Fol. | ACT/360 |
| 2M | USSOB | OIS | 2d | 2m | 1.6811 | 2m | Mod. Fol. | ACT/360 | 1y | Mod. Fol. | ACT/360 |
| 3M | USSOC | OIS | 2d | 3m | 1.698 | 3m | Mod. Fol. | ACT/360 | 1y | Mod. Fol. | ACT/360 |
| 4M | USSOD | OIS | 2d | 4m | 1.747 | 4m | Mod. Fol. | ACT/360 | 1y | Mod. Fol. | ACT/360 |
| 5M | USSOE | OIS | 2d | 5m | 1.7784 | 5m | Mod. Fol. | ACT/360 | 1y | Mod. Fol. | ACT/360 |
| 6M | USSOF | OIS | 2d | 6m | 1.8025 | 6m | Mod. Fol. | ACT/360 | 1y | Mod. Fol. | ACT/360 |
| 7M | USSOG | OIS | 2d | 7m | 1.8334 | 7m | Mod. Fol. | ACT/360 | 1y | Mod. Fol. | ACT/360 |
| 8M | USSOH | OIS | 2d | 8m | 1.8659 | 8m | Mod. Fol. | ACT/360 | 1y | Mod. Fol. | ACT/360 |
| 9M | USSOI | OIS | 2d | 9m | 1.8942 | 9m | Mod. Fol. | ACT/360 | 1y | Mod. Fol. | ACT/360 |
| 10M | USSOJ | OIS | 2d | 10m | 1.9241 | 10m | Mod. Fol. | ACT/360 | 1y | Mod. Fol. | ACT/360 |
| 11M | USSOK | OIS | 2d | 11m | 1.9533 | 11m | Mod. Fol. | ACT/360 | 1y | Mod. Fol. | ACT/360 |
| 1Y | USSO1 | OIS | 2d | 1y | 1.974 | 1y | Mod. Fol. | ACT/360 | 1y | Mod. Fol. | ACT/360 |

### 2.2.2 USD Forward Index LIBOR 3m Curve

In the previous section, we define the methodology followed for the construction of the USD discounting curve. Here if we recall the significance of this curve. This curve is used to discount every cash flow nominated in USD currency. In this section, we present the methodology for building index forward curves. We present a methodology of how to estimate the forward curve for LIBOR 3m. For the calibration of the forward index LIBOR 3m curve, we take the plain vanilla IRS as a benchmark. The maturities and swap rates that we will use for the forward curve calibration represented within the tables in the following section.

Let $PV(t)$ represents the present value (at time $t$) of a payer IRS denominated in USD based on LIBOR 3m with maturity of $y$ years, then we write

$$PV(t) =$$

$$\sum_{i=1}^{Q_y} \alpha(t_{i-1}, t_i)\, \mathbb{E}_t^{t_i}\big(\mathbf{LIBOR3M}(t_{i-1}, t_i)\big) P(t, t_i) - k_y \sum_{j=1}^{S_y} \beta\big(s_{j-1}, s_j\big)\, P\big(t, s_j\big)\,, \qquad (2.14)$$

where

$k_y$: fixed rate of the plain vanilla interest rate swap with maturity in *y* years

$Q_y$: number of quarters in *y* years

$S_y$: number of semesters in *y* years

$t_i$: coupon periods (start date, end date) for the leg indexed to LIBOR 3m

$s_i$: coupon periods (start date, end date) for the fixed leg

$\alpha(t_{i-1}, t_i)$: accrual factor of the $i$th coupon of the floating leg (ACT/360)

$\beta(s_{j-1}, s_j)$: accrual factor of the $j$th coupon of the fixed leg (30/360)

$P(t, s_j)$: discount factors in USD

$\mathbb{E}_t^{t_i}(\mathbf{LIBOR3M}(t_{i-1}, t_i))$: the LIBOR 3m forward rate of the $i$th coupon.

The above characteristics present the plain vanilla IRS in the USD market. It swaps LIBOR 3m payable quarterly versus a semiannual fixed-rate coupon with a day count of 30/360 that is used primarily in government bonds. It is referred to as the plain vanilla since it is the most standard and liquid swap in the market.

Now, let us rewrite $\mathbb{E}_t^{t_i}(\mathbf{LIBOR3M}(t_{i-1}, t_i))$ from equation $(2.15)$ in terms of a discount curve

$$\mathbb{E}_t^{t_i}(\mathbf{LIBOR3M}(t_{i-1}, t_i)) = \frac{1}{\tau(t_{\mathrm{i}-1}, t_{\mathrm{i}})}\left(\frac{P^{3m}(t, t_{i-1})}{P^{3m}(t, t_i)} - 1\right), \qquad (2.16)$$

where $\tau(t_{\mathrm{i}-1}, t_{\mathrm{i}}) = \tau_i$ represents the day count convention to determine the year fraction for the discounting and curve building.

Combining $(2.16)$ and $(2.17)$ and solving for discount factor obtained calibrated to USD LIBOR 3m, $P^{3m}\left(t, t_{Q_y}\right)$ yields

$$P^{3m}\left(t, t_{Q_y}\right) =$$

$$\frac{P^{3m}\left(t, t_{Q_y-1}\right)}{1 + \frac{\tau_{Q_y}\left(k_y \sum_{j=1}^{S_y} \beta_j P\left(t, s_j\right) - \sum_{i=1}^{Q_y-1} \frac{\alpha_i}{\tau_i}\left(\frac{P^{3m}(t, t_{i-1})}{P^{3m}(t, t_i)} - 1\right) P(t, t_i)\right)}{\alpha_{Q_y} P\left(t, t_{Q_y}\right)}}. \qquad (2.18)$$

This equation supports us in finding the discount curve based on LIBOR 3m using a simple bootstrapping and an interpolation method. In Table 2.2, market data mentioned in the estimation of USD Forward Index LIBOR 3m Curve is represented.

Table 2.2 USD Forward Index LIBOR 3m Curve Bloomberg Data. Bloomberg market data terms and conditions table referred in calibration of USD Forward Index LIBOR 3m Curve. Quotes are End of Day prices from 20/08/2018

| **Tenor** | **Bloomberg Ticker** | **Start day** | **End day** | **Rate** | **Type** | **Floating Leg Period** | **Floating Leg Business Day Rule** | **Floating Leg Business Day Count** | **Fixed Leg Period** | **Fixed Leg Business Day Rule** | **Fixed Leg Business Day Count** |
|---|---|---|---|---|---|---|---|---|---|---|---|
| ON | US00O/N | 0d | 1d | 1.45 | Cash | - | Following | ACT/360 | - | - | - |
| TN | US00T/N | 1d | 1d | 1.5 | Cash | - | Following | ACT/360 | - | - | - |
| 3M | US0003M | 2d | 3m | 2.25 | Cash | 3m | Mod. Fol. | ACT/360 | - | - | - |
| 6M | USSWF | 2d | 6m | 2.35 | IRS | 3m | Mod. Fol. | ACT/360 | 6m | Mod. Fol. | 30/360 |
| 9M | USSWI | 2d | 9m | 2.39 | IRS | 3m | Mod. Fol. | ACT/360 | 6m | Mod. Fol. | 30/360 |
| 1Y | USSW1 | 2d | 1y | 2.43 | IRS | 3m | Mod. Fol. | ACT/360 | 6m | Mod. Fol. | 30/360 |

### 2.2.3 TRY Discount Curve

Since interest rate derivatives markets is not deep in TRY, funding is performed mostly using foreign exchange swaps on interbank market of TRY. Accordingly, discount curve construction market practice is based on liquid foreign exchange instruments. Hence, in this study we benefit from foreign exchange instruments while calibrating the TRY discount curve.

For terms smaller than 1-year, foreign exchange swap quotes are fitted to discount curves. As Kazdal and Küçüksaraç states in [14], foreign exchange swaps and outright forwards are similar in nature and, moves together. In this study, assuming their finding, we take forward implied rates for calibration of TRY discount curve. Otherwise, may need to translate cross-currency-swap rates into zero coupon rates by bootstrapping.

For a 1-year term and further, cross-currency swaps are more liquidly traded rather than foreign exchange swaps in case of currency TRY. Therefore, we use 1-year cross-currency swap quotes of TRY fixed payer- USD LIBOR 3m receiver, for the long end of the curve.

OIS instruments denominated in TRY could not be used for the construction of the curve since there are no liquid quotes. Nevertheless, we can still utilize information from OIS instruments in USD. TRY discounting curve constructed in the following sections is linked to OIS discounting, as per foreign exchange instruments whose USD denominated cash flows are discounted with OIS discounting

.

#### 2.2.3.1 Short Terms of TRY Discount Curve

In this section, we form the short end of the TRY discounting curve. As stated in previous section, we take forward implied rates for tenors shorter than 1-year. Present value of a forward contract is

$$PV(t) = \mathbb{E}_t^{t_i}(\mathbf{USD})P_{TRY}(t,t_i) - kP_{TRY}(t,t_i)\,, \tag{2.19}$$

where $t_i$ is the maturity date of outright forward contract and, $P_{TRY}(t,t_i)$ is the discount factor for TRY nominated instruments and $k$ is the mid-market quote for outright contract.

By interest rate parity, there is a strong relationship between forward rates and interest rates that is given by

$$\mathbb{E}_t^{t_i}(\mathbf{USD}) = S_t\,\frac{P(t,t_i)}{P_{TRY}(t,t_i)}, \tag{2.20}$$

where $P(t,t_i)$ is discount factor for USD nominated instruments and $S_t$ is todays spot exchange rate to buy USD for TRY. Thus, $P(t,t_i)$ acquired from OIS calibration links our TRY discount curve to OIS discounting framework. Substituting equation (2.20) into (2.19),

$$PV(t) = S_t\,P(t,t_i) - kP_{TRY}(t,t_i)\,. \tag{2.21}$$

Now, if we assume that the fixed rate $k$ is a mid-market quote then, again, by the no-arbitrage arguments we have the result that the present value of the outright forward amounts to zero. Therefore,

$$P_{TRY}(t,t_i) = \frac{S_t P(t,t_i)}{k}\,. \tag{2.22}$$

However, we still should interpret (2.22) as our market data, namely in terms of swap points and spot rate at spot date we have

$$P_{TRY}(t,t_i) = \frac{\left(S_{t_0} + \frac{F(t,\text{TOD})}{10{,}000}\right) P(t,t_i)}{\left(S_{t_0} + \frac{F(t_0,t_i)}{10{,}000}\right)}, \qquad (2.23)$$

where,

$S_{t_0}$: spot exchange rate to buy USD for TRY at spot date, the next business date.

$F(t,\text{TOD})$: negative swap point to discount spot rate from spot date to today with basis equal to 10,000

$F(t_0,t_i)$: positive swap point to compound spot rate from spot date to $t_i$ with basis equal to 10,000

$t_i$: Maturity date of outright forward contract

$P(t,t_i)$: discount factor in USD (estimated using OIS instruments)

Thus, TRY discount factors are estimated for some specific tenors up to 9 months. We have directly used swap points and a USD discount factors. OIS discounting framework have been employed by using $P(t,t_i)$ which is taken from OIS based yield curve that we have constructed in section 2.2.1. However, we will need another yield curve to estimate the last remained tenor in TRY discount curve construction.

#### 2.2.3.2 1-year Tenor of TRY Discount Curve

In this section, we have derived a formula for the long end of the TRY discount curve. Let us refer to index forward rates from the previous section in order to describe how to estimate the forward curve for LIBOR 3m. For the construction of the long-end of TRY discounting curve, we use cross-currency swap quotes. In tables, we present the maturities and swap rates that we will use for the discount curve calibration.

Let $PV(t)$ be the present value of a TRY fixed rate payer- USD LIBOR 3m receiver cross-currency swap denominated in USD based on LIBOR 3m with a maturity of *y* years, hence.

$$\begin{aligned} PV(t) \;=\; & \sum_{i=1}^{Q_y} \alpha(t_{i-1}, t_i)\, \mathbb{E}_t^{t_i}\big(\mathbf{LIBOR3M}(t_{i-1}, t_i)\big) P(t, t_i) \\ & - \; k_y \sum_{j=1}^{S_y} \beta\big(s_{j-1}, s_j\big)\, P_{TRY}\big(t, s_j\big)\,, \end{aligned} \tag{2.24}$$

where

$k_y$: TRY fixed rate of the cross currency swap with maturity in *y* years

$Q_y$: number of quarters in *y* years

$S_y$: er of semesters in *y* years

$t_i$: coupon periods (start date, end date) for the leg indexed to LIBOR 3m

$s_i$: coupon periods (start date, end date) for the fixed leg

$\alpha(t_{i-1}, t_i)$: accrual factor of the $i$th coupon of the floating leg (ACT/360)

$\beta\big(s_{j-1}, s_j\big)$ accrual factor of the $j$th coupon of the fixed leg (ACT/360)

$P(t, s_j)$: discount factors in USD (estimated using OIS instruments)

$\mathbb{E}_t^{t_i}(\mathbf{LIBOR3M}(t_{i-1}, t_i))$: the USD LIBOR 3m forward rate of the $i$th coupon.

This cross-currency swap with the above characteristics is the most liquid swap in the market. It exchanges USD LIBOR 3m payable quarterly versus an annual TRY fixed rate coupon with a day count of ACT/360. Namely, have taken the number of days in subjected period and divide it by 360.

Substituting (2.16) into and solving for $P^{3m}\left(t, t_{Q_y}\right)$ yields,

$$P_{TRY}\left(t, s_{S_y}\right) = \frac{\sum_{i=1}^{Q_y}\left(\frac{P^{3m}(t,t_{i-1})}{P^{3m}(t,t_i)} - 1\right)P(t,t_i) - k_y\sum_{j=1}^{S_y-1}\beta_j\, P_{TRY}(t,s_j)}{k_y\beta_{S_y}}. \tag{2.25}$$

For our long-end case, when $S_y = 1$ and $Q_y = 4$ we obtain

$$P_{TRY}\left(t, s_{S_y}\right) = \frac{\sum_{i=1}^{4}\left(\frac{P^{3m}(t,t_{i-1})}{P^{3m}(t,t_i)} - 1\right)P(t,t_i)}{k_y\beta_{S_y}}, \tag{2.26}$$

where $P^{3m}(t, t_i)$ is the discount factor obtained from USD LIBOR 3m forward index curve. This equation together with (2.23) allows us to find TRY discount curve based on FX swaps and CIRS using a simple bootstrapping and an interpolation method.

In a few words, in this section, we have aimed to construct zero coupon curves to benefit in the option pricing procedure. Risk-neutral valuation requires risk-free estimates of discount factor, so we applied for the instruments that are accepted to converge the risk-free proxy. However, those instruments are quoted for some specific

time period which may not starts from today. We cannot directly use quotes unless their "Type" column in Table 2.2 and Table 2.3 are not equal to "Cash". We have benefited cash instruments for discounting the later instruments (which have start day greater than 0) to today which have start day greater than 0. By this way we have achieved the zero-coupon rates for each "End day" in these tables. Besides, in these tables, non-empty cells of in column "Floating Leg Period" implies that the instrument has a floating leg. Namely, we should consult to another yield curve to obtain estimated fixed values of that period. In this manner we have built USD LIBOR 3m Curve and also studied section "1-year Tenor of TRY Discount Curve" as byproducts.

Table 2.3: TRY Discount Curve Bloomberg Data. Bloomberg market data terms and conditions table referred in calibration of TRY Discount Curve. Quotes are End of Day prices from 20/08/2018

| Tenor | Type | Bloomberg Ticker | Start day | End day | Rate | Floating Leg Period | Floating Leg Business Day Rule | Floating Leg Business Day Count | Fixed Leg Period | Fixed Leg Business Day Rule | Fixed Leg Business Day Count |
|---|---|---|---|---|---|---|---|---|---|---|---|
| TOD | Forward | TRYTOD | 1d | 0d | -12.00000 | - | Following | ACT/360 | - | - | - |
| ON | Forward | TRYON | 0d | 1d | 12.00000 | - | Following | ACT/360 | - | - | - |
| 1W | Forward | TRY1W | 1d | 1w | 81.95000 | 1y | Following | ACT/360 | 1y | Following | ACT/360 |
| 2W | Forward | TRY2W | 1d | 2w | 162.00000 | 1y | Following | ACT/360 | 1y | Following | ACT/360 |
| 3W | Forward | TRY3W | 1d | 3w | 241.64000 | 1y | Following | ACT/360 | 1y | Following | ACT/360 |
| 1M | Forward | TRY1M | 1d | 1m | 390.68000 | 1y | Following | ACT/360 | 1y | Following | ACT/360 |
| 2M | Forward | TRY2M | 1d | 2m | 704.50000 | 1y | Following | ACT/360 | 1y | Following | ACT/360 |
| 3M | Forward | TRY3M | 1d | 3m | 1066.25000 | 1y | Following | ACT/360 | 1y | Following | ACT/360 |
| 4M | Forward | TRY4M | 1d | 4m | 1449.07000 | 1y | Following | ACT/360 | 1y | Following | ACT/360 |
| 5M | Forward | TRY5M | 1d | 5m | 1871.02000 | 1y | Following | ACT/360 | 1y | Following | ACT/360 |
| 6M | Forward | TRY6M | 1d | 6m | 2184.50000 | 1y | Following | ACT/360 | 1y | Following | ACT/360 |
| 9M | Forward | TRY9M | 1d | 9m | 3358.55000 | 1y | Following | ACT/360 | 1y | Following | ACT/360 |
| 1Y | CIRS | TYUSSW1 | 2d | 1y | 12.38000 | 3m | Mod. Fol. | ACT/360 | 1y | Following | ACT/360 |

In Figure 2.2 we present estimated yield curves (TRY Discount Curve, USD Discount Curve, LIBOR 3m Forward Curve) for date 20/08/2018. We have observed that LIBOR 3m Index Curve is higher than OIS based yield curve at all tenors. This means that there is a non-negative spread between the LIBOR 3m Forward Curve and USD Discount Curve.

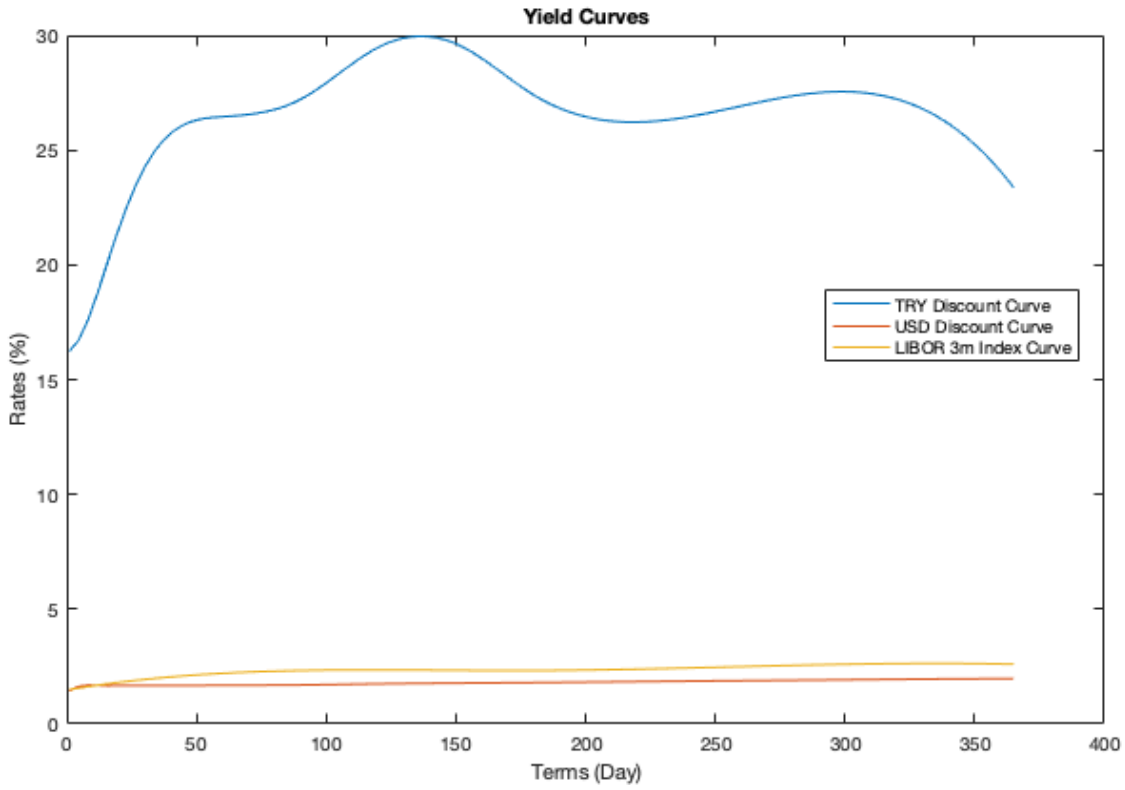


Figure 2.2: Yield Curves Estimated at Date 20/08/2018.

# CHAPTER 3

# MODELS

## 3.1 Black Scholes Model

In 1973 Black and Scholes derived the price of European call and put options. In 1983 Garman et al implemented Black-Scholes approach to foreign exchange options, see details in [6].

Here if we let $S_t$ to be the spot rate, i.e., the amount of money in the domestic currency required to buy one unit of foreign currency. Assumption accepted for the model is that the spot exchange rate adopts a geometric Brownian motion, and further, not an only domestic risk-free asset ($B_d$) but also a foreign risk-free asset ($B_f$) with constant interest rates are considered:

$$dS_t = S_t \mu dt + S_t \sigma d\bar{W} \tag{3.1}$$

$$dB_d = r_d B_d dt \tag{3.2}$$

$$dB_f = r_f B_f dt\,, \tag{3.3}$$

where $\bar{W}$ is a Wiener process under market probability measure $\mathbb{P}$.

Björk et al. derived a formula for $dS_t$ in terms of a wiener process of a risk-neutral measure, (see [3] for details):

$$S_t = S_0 e^{\left(r_d - r_f - \frac{1}{2}\sigma^2\right)t + \sigma W_t}. \quad (3.4)$$

### 3.1.1 Option Pricing Formula

In foreign exchange markets, most of the options are subject to physical settlement (i.e., taking long position in USDTRY vanilla call indicates being entitled to receive USD notional amount $N$ at maturity and pay ($N \times K$)TRY, where $K$ is the strike price). The price of such instrument is calculated with the Black–Scholes formula,

$$H(S_t, K, \sigma, \phi) = \phi[S_t e^{-r_f \tau} N(\phi d_+) - e^{-r_d \tau} K N(\phi d_-)] \quad (3.5)$$

$$= \phi e^{-r_d \tau}[f(t,T) N(\phi d_+) - K N(\phi d_-)], \quad (3.6)$$

where $f(t,T)$ denones forward rate, $d_\pm = \frac{\ln\frac{f(t,T)}{K} \pm \frac{1}{2}\sigma^2\tau}{\sigma\sqrt{\tau}}$, $\phi$ denotes call options if it equals to $+1$ and denotes put options if it equals to $-1$, $K$ is the option's strike price, $\sigma$ denotes implied volatility (by the Black-Scholes model) and $N(x)$ is the cumulative distribution function of the standard normal distribution. (See details in Wystup et al. [19])

### 3.1.2 Adjusted Black-Scholes Option Pricing

Despite the advanced models proposed in the literature, the Black-Scholes model commonly accepted by market practitioners. The practitioners build a volatility surface

to use it as $\sigma$ in the Black-Scholes model. Namely, the market practitioners do not use a constant coefficient $\sigma$ in the Black-Scholes model.

The market practitioners construct the volatility surface by linear interpolation of the market quotation of implied volatilities. Therefore, they are violating the assumption constant volatility of the Black-Sholes model and they are exposed to any losses from being arbitraged.

We will use the formula below to find the interpolated market implied volatilities.

$$\bar{\sigma}(K,\tau_i) = \sigma_{market}(K,\tau_{i-1}) + (\tau_i - \tau_{i-1})\frac{\sigma_{market}(K,\tau_{i+1}) - \sigma_{market}(K,\tau_{i-1})}{\tau_{i+1} - \tau_{i-1}}. (3.7)$$

## 3.2 Heston Model

In option pricing theory, Black Scholes in [4] bring a formula that option prices are associated with the distribution of underlying. While the option pricing formula of Black and Scholes was outstanding by describing the distribution of underlying prices and option price dynamic. Moreover, Black and Scholes did not consider the smile effect is not considered in the model assumptions. Namely, options with varying exercise prices and time-to-maturities does not necessarily produce different implied volatilities, due to the constant volatility assumption. In case the market prices of options are reversed with the Black-Scholes formula to get volatility, with given exercise price, time-to-maturity, discount rate, and underlying price, it is entitled Black Sholes implied-volatility. This case is inconsistent with the assumption that the underlying price process involves

constant volatility because it has been noticed that options with the same underlying but with different exercise prices and time-to-maturities indeed comprise varying volatilities. A simple solution for this issue is to govern varying models per different strike prices and time-to-maturities, in order that these models would produce varying volatilities over strike-axis and time-to-maturity axis. Nevertheless, employing varying models could lead to divergence on the handling of option portfolios that consists of different strike prices and time-to-maturities.

Eventually, the literature focused on to mitigate the constant volatility assumption. The recent improvement of the literature has brought forth models with local volatility. Merton et al. in [17] proposed that building the volatility related to time-to-maturity. While this proposal describes the varying implied volatilities over time, it could not adequately analyze the volatility smile over different strikes. Dupire et al. in [8], and Rubinstein et al. in [20] suggest designing the volatility as a variable with respect to time, and also to state variables. Their perspective was adequate to produce the volatility smile, yet it falls to produce continuous smile behavior, which does not dissolve across time-period.

Local volatility models led the approach of designing the volatility as a stochastic process with their deficiency. The following development is the study of Scott [21], Hull and White [11], and Wiggins [22]. Their design of stochastic volatility is more advanced than the Local Volatility Model. However, stochastic volatility models' disadvantages are the deficiency of having analytic solutions for European options and significant dependency of numerical techniques.

The stochastic volatility model Heston [10] is distinct from the others. Firstly, the Heston model involves a stochastic variance process, which is mean-reverting and non-negative, in line with the market. The second reason is that the Heston model involves a semi-closed formula for the solution European options, whose implementation is simple. Yet another advantage is prominent in model calibration to the market data. Thus, these capabilities led Heston's model to be well-known, and many professionals benefit from this model in many applications, such as treasury software implementation.

### 3.2.1 Definition

Heston in [10], introduced the following model:

$$\begin{aligned} dS_t &= \mu S_t dt + \sqrt{V_t} S_t dW_t^1 \\ dV_t &= \kappa(\theta - V_t)dt + \sigma\sqrt{V_t} S_t dW_t^2 \\ dW_t^1 dW_t^2 &= \rho dt \,, \end{aligned} \tag{3.8}$$

where $S_t$ and $V_t$ denote the spot price and variance processes, respectively. $W_t^1$ and $W_t^2$ are Brownian motions with the correlation coefficient $\rho$. Here, $\mu$ is the expected rate of return of the underlying asset. $\theta$ is the long-term mean of the variance process, $\kappa$ is the speed of the mean reversion of the variance process; and $\sigma$ stands for the volatility of the variance process.

In case of $\rho > 0$, the price process becomes more volatile as the underlying price or returns increase. Oppositely, in case of $\rho < 0$, the price process becomes more volatile as the underlying price or returns decrease. The correlation coefficient $\rho$, then, influence

the skewness of the distribution. If $\sigma$ equals to 0, then the second Brownian motion will be removed so that the volatility becomes deterministic. Hence, the log-returns are distributed normally. Bigger $\sigma$ lead the skew/smile evident. Namely, volatility becomes volatile further. On the other hand, $\kappa$, the mean reversion parameter $\kappa$ could be explained as describing the degree of volatility clustering. This behavior is in line with the market; large price variations expected to result in significant price variations.

### 3.2.2 Option Pricing Formula

Risk neutral valuation considers contingent claim pricing under equivalent martingale measure. The price is calculated as the expected discounted payoff of the contingent claim, in the equivalent martingale measure $\mathbb{Q}$ [5]. Hence,

$$H\left(\kappa, \theta, \sigma, \rho, \lambda, r_d, r_f, v_t, S_t, K, \tau, \phi\right) = \mathbb{E}_t^Q\left[e^{r(T-t)}H(T)\right], \tag{3.9}$$

where *H(T)* denotes the payoff of the option at time *T* and *r* denotes the risk-free rate across [t, T]. Shifting from a physical measure to equivalent martingale measure is obtained by Girsavov's theorem. Especially

$$\begin{aligned} d\widetilde{W}_t^1 &= dW_t^1 + v_t dt \\ d\widetilde{W}_t^2 &= dW_t^2 + \Lambda(S,V,t)dt \\ \frac{d\mathbb{Q}}{d\mathbb{P}} &= exp\left\{-\frac{1}{2}\int_0^t v_s^2 + \Lambda(S,V,s)ds - \int_0^t v_s dW_s^1 - \int_0^t \Lambda(S,V,t)dW_t^2\right\} \qquad (3.10) \\ v_t &= \frac{\mu - r}{\sqrt{V_t}}, \end{aligned}$$

where $\mathbb{P}$ denotes the physical measure and $\widetilde{W}_t^1$ and $\widetilde{W}_t^2$ are $\mathbb{Q}$-Brownian motions. $\lambda = \lambda(t, v, S)$ referred as the volatility risk premium. In measure $\mathbb{Q}$, (3.8) is

$$\begin{aligned} dS_t &= rS_t dt + \sqrt{V_t} S_t d\widetilde{W}_t^1 \\ dV_t &= \kappa^*(\theta^* - V_t)dt + \sigma\sqrt{V_t} S_t d\widetilde{W}_t^2 \\ d\widetilde{W}_t^1 d\widetilde{W}_t^2 &= \rho dt\,, \end{aligned} \tag{3.11}$$

where,

$$\begin{aligned} \kappa^* &= \kappa + \lambda \\ \theta^* &= \frac{\kappa\theta}{\kappa + \lambda}. \end{aligned} \tag{3.12}$$

We will assume $\lambda$=0. In a complete market, every asset/option corresponds to the same market price of risk. Yet volatility lacks direct information about itself since it is not a traded asset. Hence this yields incomplete market and, $\lambda(t, v, S)$ is not a constant. It is apparent that (3.10) solely impose the equivalent martingale measure. This yields the equivalent martingale measure to be not unique and be dependent on the value of $\lambda(t, v, S)$. Various equivalent martingale measures will generate various option prices, depending on the choice of $\lambda(t, v, S)$. At first, this could point out an issue. However, the issue is defeated because of the parametric nature of the model and the existence of a closed-form solution.

Therefore, our risk neural-measure and physical measure is the same. With this assumption, we will refer derivation of the closed form solution in following paragraphs.

Suppose a contingent claim, whose value is $G(t, v, S)$ at time $t$, paying $G(T, v, S)$ at time $T$. Because Heston model employs two Brownian motions, the self-financing

portfolio must involve the probabilities of the money market, spot market and a derivative instrument whose value is $V(t, v, S)$ . The differential of the wealth process $X$ is given by:

$$dX = \Delta dS + \Gamma dV + r_d(X - \Gamma V - \Delta S)dt + r_f \Delta S dt\,, \tag{3.13}$$

where Δ denotes the amount of underlying held and Γ denotes the amount of derivative instruments $V$, at time $t$. Our goal is establishing a portfolio whose initial value is $X_0$, and solving for Δ and Γ to have $X_t = G(t, v, S)$ for all $t = [0, T]$. The popular technique is examining the differential of $X$ and $G$. A few calculations lead the partial differential equation which G must solve, in order to avoid the arbitrage:

$$\begin{aligned} &\frac{1}{2} v S^2 \frac{\partial^2 G}{\partial S^2} + \rho\sigma v S \frac{\partial^2 G}{\partial S \partial v} + \frac{1}{2}\sigma^2 v \frac{\partial^2 G}{\partial v^2} + (r_d - r_f) S \frac{\partial G}{\partial S} \\ &\qquad + \{\kappa(\theta - v) - \lambda(t, v, S)\} \frac{\partial G}{\partial v} + \frac{\partial G}{\partial t} - r_d G = 0\,. \end{aligned} \tag{3.14}$$

Here we recall that $\lambda(t, v, S)$ represents the volatility risk premium and different levels of $\lambda(t, v, S)$ would result in different risk-neutral measure and yields an incomplete market. Nevertheless, this is in the nature of Heston model, because the model has one more independent equation, Brownian motion for the variance process, in contrast to simpler models. For solving the partial differential equation above, the appropriate boundary conditions must be governed. The conditions for European options are given by

$$G(T, v, S) = max\{\phi(S - K), 0\} \tag{3.15}$$

$$G(t, v, 0) = \frac{1 - \phi}{2} K e^{-r_d \tau} \tag{3.16}$$

$$\frac{\partial G}{\partial S}(t,v,\infty) = \frac{1+\phi}{2}e^{-r_f\tau} \tag{3.17}$$

$$r_d G(t,0,S) = \left(r_d - r_f\right)S\frac{\partial G}{\partial S}(t,0,S) + \kappa\theta\frac{\partial G}{\partial v}(t,0,S) + \frac{\partial G}{\partial t}(t,0,S) \tag{3.18}$$

$$G(t,\infty,S) = \begin{cases} Se^{-r_f\tau} & \phi = +1 \\ Ke^{-r_d\tau} & \phi = -1 \end{cases}, \tag{3.19}$$

where $K$ denotes the exercise price, $\phi$ specifies call options if $\phi = 1$ and put options if $\phi = -1$, and $\tau = T - t$ stands for the time-to-maturity. Heston proposed the solution of the partial differential equation for European type currency option price as follows, see also [13]:

$$H\left(\kappa,\theta,\sigma,\rho,\lambda,r_d,r_f,v_t,S_t,K,\tau,\phi\right) = \phi\{Se^{-r_f\tau}P_+(\phi) - Ke^{-r_d\tau}P_-(\phi)\}, \tag{3.20}$$

where $u_{1,2} = \pm\frac{1}{2}$, $b_1 = \kappa + \lambda - \sigma\rho$, $b_2 = \kappa + \lambda$, and,

$$d_{\mathrm{j}} = \sqrt{(\rho\sigma\varphi i - b_j)^2 - \sigma^2(2u_j\varphi i - \varphi^{2)}} \tag{3.21}$$

$$g_{\mathrm{j}} = \frac{b_j - \rho\sigma\varphi i + d_j}{b_j - \rho\sigma\varphi i - d_j} \tag{3.22}$$

$$C_j(\tau,\varphi) = \left(r_d - r_f\right)\varphi i\tau + \frac{\kappa\theta}{\sigma^2}\left\{\left(b_j - \rho\sigma\varphi i + d_j\right)\tau - 2\log\left(\frac{1-g_j e^{d_j\tau}}{1-g_j}\right)\right\} \tag{3.23}$$

$$D_j(\tau,\varphi) = \frac{b_j - \rho\sigma\varphi i + d_j}{\sigma^2}\left(\frac{1-e^{d_j\tau}}{1-g_j e^{d_j\tau}}\right) \tag{3.24}$$

$$f_j(x,v_t,\tau,\varphi) = exp\{C_j(\tau,\varphi) + D_j(\tau,\varphi)v_t + i\varphi x\} \tag{3.25}$$

$$P_j(x,v_t,\tau,y) = \frac{1}{2} + \frac{1}{\pi}\int_0^\infty \Re\left\{\frac{e^{-\mathrm{i}\varphi y}f_j(x,v_t,\tau,\varphi)}{i\varphi}\right\} d\varphi\,. \tag{3.26}$$

The functions $P_j$ denote the cumulative distribution functions (of variable $y = \log K$) of the logarithm of the spot price after time $\tau = T - t$ starting at $x = \log S_t$ for some trend $\mu$. Thus:

$$P_+(\phi) = \frac{1-\phi}{2} + \phi P_1(x, v_t, \tau, y) \tag{3.27}$$

$$P_-(\phi) = \frac{1-\phi}{2} + \phi P_2(x, v_t, \tau, y)\,. \tag{3.28}$$

### 3.2.3 Computational issues

The solution that Heston suggests is semi-analytical. $P_+(\phi)$ and $P_-(\phi)$ defined by (3.27) and (3.28) involve integrand functions $f_j$, that generally have oscillating characteristics, in [13]. have recommended performing an elementary transformation during the calculation of the characteristic function. They have also demonstrated that the stability of the derived formulas is provided on a full-dimensional and unlimited parameter range. Meaning that the solution uses the following instead of $g_j$,

$$\tilde{g}_j = \frac{1}{g_j} = \frac{b_j - \rho\sigma\varphi i - d_j}{b_j - \rho\sigma\varphi i + d_j}, \tag{3.29}$$

which yields to new formulas for $C_j$ and $D_j$; respectively

$$C_j(\tau, \varphi) = \left(r_d - r_f\right)\varphi i\tau + \frac{\kappa\theta}{\sigma^2}\left\{\left(b_j - \rho\sigma\varphi i - d_j\right)\tau - 2\log\left(\frac{1-\tilde{g}_j e^{-d_j\tau}}{1-\tilde{g}_j}\right)\right\} \tag{3.30}$$

and,

$$D_j(\tau, \varphi) = \frac{b_j - \rho\sigma\varphi i - d_j}{\sigma^2}\left(\frac{1-e^{-d_j\tau}}{1-\tilde{g}_j e^{-d_j\tau}}\right). \tag{3.31}$$

These are to be used in (3.25). Here we emphasize the minor differences in (3.22) and (3.29), (3.31), (3.24) and (3.31), respectively. The only difference per pair is flipped plus or minus signs in front of the $d_j$'s. The inconvenience due to referring (3.22)-(3.24) is negligible. Actually, in case of short or middle term maturities are taken into consideration on valuation and back-testing, the problem might not be captured at all. Nonetheless, if longer maturities are considered (basically, 3-5 years or longer), results diverse drastically and, absolute threshold depends on parameters, for a detailed explanation, we refer to Albrecher et al. and Janek et al. [1], [13].

### 3.2.4 Feller Condition

The Cox-Ingersoll-Ross process for the variance, formulated by (3.8), is strictly positive. Such feature is remarkable, and yields results in line with the market. Nevertheless, optimally we require a strictly positive variance process, alternatively the underlying process converge to a deterministic function when variance process falls near to zero. To ensure the variance to be strictly positive, we would set condition that

$$\alpha := \frac{4\kappa\theta}{\sigma^2} \geq 2\,, \tag{3.32}$$

which is often called as the Feller condition.

Unfortunately, during estimation of the Heston model with market option prices, parameters that violate the Feller condition (3.32) are not rare. This is not an exhaustive trouble, since it is only infinitesimally small amount of time for the variance process to strike zero, yet it would be concerning that very low levels of volatility (e.g. say below

1%) are repeatedly reached for short amounts of time and that is not something observed in the market. In addition to it is crucial for modeling approach, the Feller condition is a subject in computational efficiency. During Monte Carlo simulations Feller condition should also be considered in order that the simulation paths is strictly positive in case (3.32) is not met. Considering the option PDE, the Feller condition decides either the boundary of zero-variance is in- or out-flowing, namely, either the convection vector at the boundary points in- or outwards.

By writing the log-spot transformed Heston PDE in convection-diffusion form, we have

$$\frac{\partial}{\partial t}U = div(A\ grad\ U) - div(Ub) + f\ . \tag{3.33}$$

Thus, we obtain

$$b(x,v) = v\begin{pmatrix} \frac{1}{2} \\ \kappa + \lambda \end{pmatrix} + \begin{pmatrix} \frac{1}{2}\rho\sigma + r_f - r_d \\ \frac{1}{2}\sigma^2 - \kappa\theta \end{pmatrix}, \tag{3.34}$$

which is out-flowing at $v = 0$, boundary if

$$\frac{1}{2}\sigma^2 - \kappa\theta < 0\ . \tag{3.35}$$

This is the Feller condition (3.32) is again.

# CHAPTER 4

# DATA and CALIBRATION

## 4.1 Data

### 4.1.1 Description

Data we use in this thesis has taken the vanilla option data from Bloomberg, which involves bids on at-the-money, risk-reversals, and butterflies for USDTRY. Our data consists of liquid instruments whose delta either 0.10 or 0.25. So, our options data consist of quotes ATM, 25RR, 10RR, 25BF, and 10BF. Then we would like to resolve which implied volatilities would be mapped to call or put options. Substituting (2.5) with (2.6) can obtain a general formula for delta-call and delta-put:

$$\sigma_{\Delta call} = \sigma_{\Delta BF} + \frac{1}{2}\sigma_{\Delta RR} + \sigma_{ATM}\,, \tag{4.1}$$

$$\sigma_{\Delta put} = \sigma_{\Delta BF} - \frac{1}{2}\sigma_{\Delta RR} + \sigma_{ATM}\,. \tag{4.2}$$

By this the delta basis put-call parity, we are now able to form five different on deltas for point in volatility surface. For instance, we can obtain $\sigma_{10\,\Delta call}$ and $\sigma_{10\Delta put}$ from

(4.1) and (4.2) by using 10BF,10RR and ATM. We should find the corresponding stike price for instance for $\sigma_{10\,\Delta call}$. Since our calibration method requires market implied volatilities in terms of strike prices and time-to-maturity, we benefit equation (2.3) to translate the deltas and volatilities to find the strike prices.

The market data contain daily quotes from 11 March 2013 to 20 August 2018. For each day in that period, ATM, 25RR, 10RR, 25BF and 10BF quotes are taken for terms 1-month, 2-month, 3-month, 6-month, 9-month and 12-month. For the sake of simplicity only mid-volatilities (i.e. the average of the bid and the ask implied volatilities) have been subjected in calibration phase. It is the market practice to take mid-volatilities; yet it seems interesting, because volatility and price have no linear relation.

Interest rates have been obtained as described in previously for tenors of implied volatility data requires. Bloomberg tickers listed in Table 4.1

Spot Lag refers to number of dates between the valuation date an settlement date of option quotes.

Table 4.1 Implied Volatility Sample Data. Bloomberg market data terms and conditions table referred in calibration and performance measuring for the Black-Scholes and the Heston model. Quotes are End of Day prices from 20/08/2018

| Tenor | Bloomberg Ticker | Type | Delta | Spot Lag | Rate | Business Day Rule | Business Day Count |
|---|---|---|---|---|---|---|---|
| 1M | USDTRYV1M | At the Money | 50 | 1d | 45.7175 | Mod. Fol. | ACT/360 |
| 1M | USDTRY25R1M | Risk Reversal | 25 | 1d | 17.46 | Mod. Fol. | ACT/360 |
| 1M | USDTRY10R1M | Risk Reversal | 10 | 1d | 9.6575 | Mod. Fol. | ACT/360 |
| 1M | USDTRY25B1M | Butterfly | 25 | 1d | 1.495 | Mod. Fol. | ACT/360 |

| Tenor | Bloomberg Ticker | Type | Delta | Spot Lag | Rate | Business Day Rule | Business Day Count |
|---|---|---|---|---|---|---|---|
| 1M | USDTRY10B1M | Butterfly | 10 | 1d | 4.0475 | Mod. Fol. | ACT/360 |
| 2M | USDTRYV2M | At the Money | 50 | 1d | 40.2275 | Mod. Fol. | ACT/360 |
| 2M | USDTRY25R2M | Risk Reversal | 25 | 1d | 18.0375 | Mod. Fol. | ACT/360 |
| 2M | USDTRY10R2M | Risk Reversal | 10 | 1d | 9.8475 | Mod. Fol. | ACT/360 |
| 2M | USDTRY25B2M | Butterfly | 25 | 1d | 1.5875 | Mod. Fol. | ACT/360 |
| 2M | USDTRY10B2M | Butterfly | 10 | 1d | 4.12 | Mod. Fol. | ACT/360 |
| 3M | USDTRYV3M | At the Money | 50 | 1d | 37.085 | Mod. Fol. | ACT/360 |
| 3M | USDTRY25R3M | Risk Reversal | 25 | 1d | 18.1175 | Mod. Fol. | ACT/360 |
| 3M | USDTRY10R3M | Risk Reversal | 10 | 1d | 9.8 | Mod. Fol. | ACT/360 |
| 3M | USDTRY25B3M | Butterfly | 25 | 1d | 1.665 | Mod. Fol. | ACT/360 |
| 3M | USDTRY10B3M | Butterfly | 10 | 1d | 4.2725 | Mod. Fol. | ACT/360 |
| 6M | USDTRYV6M | At the Money | 50 | 1d | 32.8175 | Mod. Fol. | ACT/360 |
| 6M | USDTRY25R6M | Risk Reversal | 25 | 1d | 18.135 | Mod. Fol. | ACT/360 |
| 6M | USDTRY10R6M | Risk Reversal | 10 | 1d | 9.8475 | Mod. Fol. | ACT/361 |
| 6M | USDTRY25B6M | Butterfly | 25 | 1d | 1.8725 | Mod. Fol. | ACT/362 |
| 6M | USDTRY10B6M | Butterfly | 10 | 1d | 4.555 | Mod. Fol. | ACT/363 |
| 9M | USDTRYV9M | At the Money | 50 | 1d | 30.75 | Mod. Fol. | ACT/364 |
| 9M | USDTRY25R9M | Risk Reversal | 25 | 1d | 18.52 | Mod. Fol. | ACT/365 |
| 9M | USDTRY10R9M | Risk Reversal | 10 | 1d | 9.9225 | Mod. Fol. | ACT/366 |
| 9M | USDTRY25B9M | Butterfly | 25 | 1d | 1.9725 | Mod. Fol. | ACT/367 |
| 9M | USDTRY10B9M | Butterfly | 10 | 1d | 4.835 | Mod. Fol. | ACT/368 |
| 1Y | USDTRYV1Y | At the Money | 50 | 1d | 29.83 | Mod. Fol. | ACT/369 |
| 1Y | USDTRY25R1Y | Risk Reversal | 25 | 1d | 18.94 | Mod. Fol. | ACT/370 |
| 1Y | USDTRY10R1Y | Risk Reversal | 10 | 1d | 10.0525 | Mod. Fol. | ACT/371 |
| 1Y | USDTRY25B1Y | Butterfly | 25 | 1d | 2.0525 | Mod. Fol. | ACT/372 |
| 1Y | USDTRY10B1Y | Butterfly | 10 | 1d | 4.935 | Mod. Fol. | ACT/373 |

### 4.1.2 Analysis

This section examines spot exchange rate USDTRY historical data, from period between 11 March 2013 and 20 August 2018. In Figure 4.1 and Figure 4.2, spot rate and daily log returns for the period are depicted respectively. We have observed that the daily log returns are higher, in absolute terms, in the recent currency crisis (The diplomatic tension between Turkey and the United States due to the detention of the pastor, Andrew Brunson), indicating a volatile market.

In Figure 4.3 a histogram of distribution of the daily log returns is presented. Red-colored curve denotes a normal probability density fitted to the daily log returns. We have also presented normal probability plot of daily log returns in Figure 4.4.

In Figure 4.3, we have observed that the occurrences is more intense in the center, and the tails are fatter than implied by the normal distribution assumption. He we emphasize the fat tails on normal probability plot of daily log returns in Figure 4.4. This, and because volatility evolves overtime implies the opposite of the crucial assumptions in the Black-Scholes model.

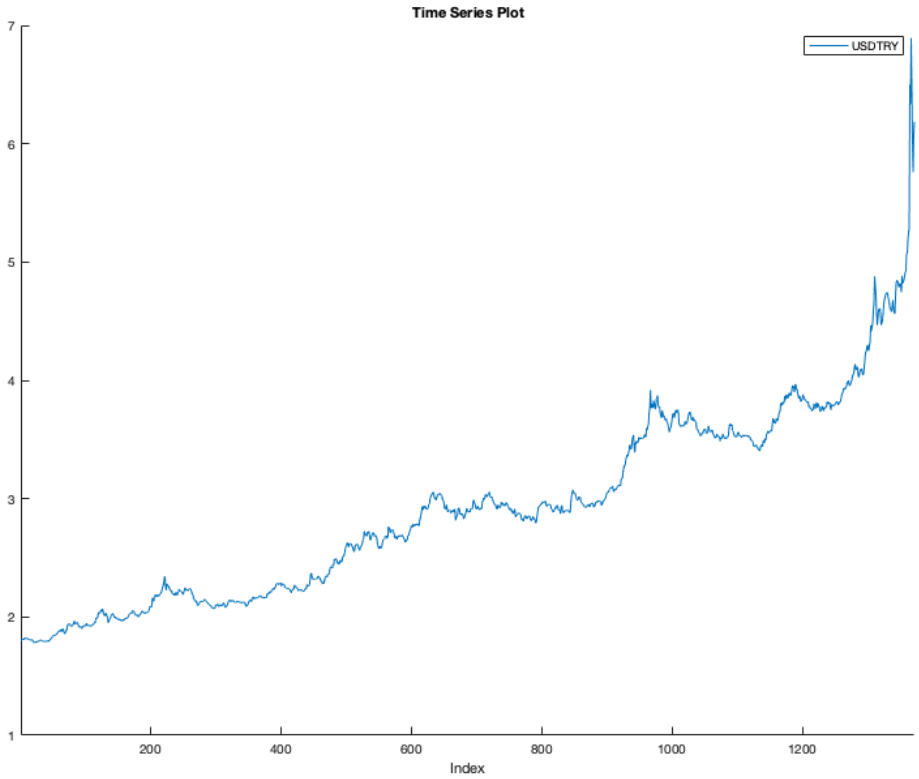

Figure 4.1: USDTRY Spot Rates Over Time Period 2013 – 2018

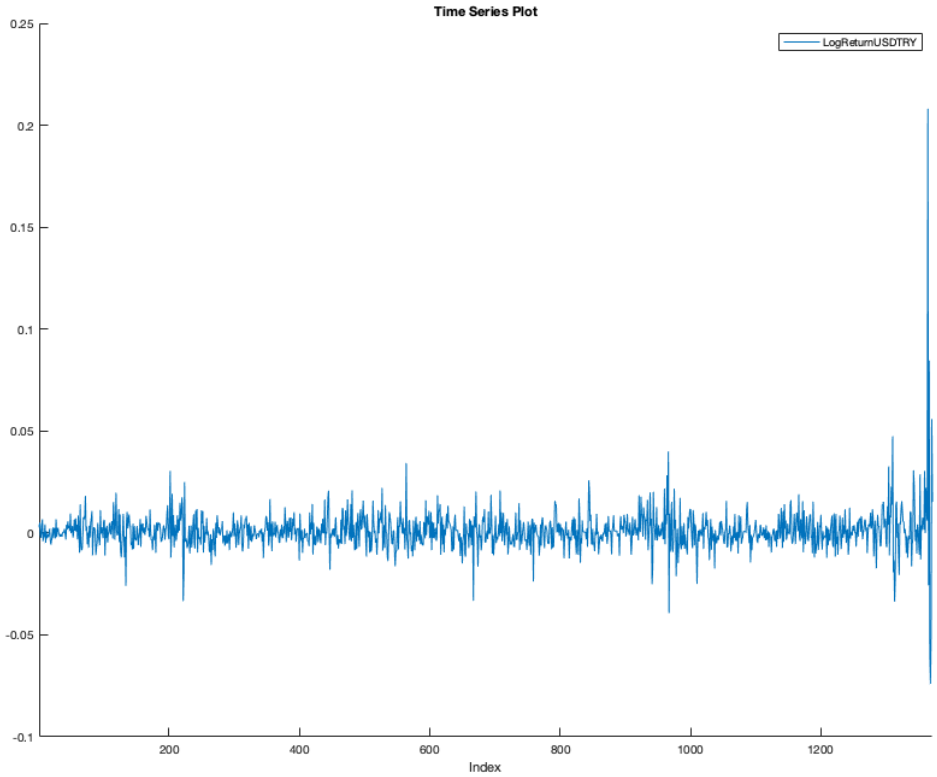

Figure 4.2: USDTRY Daily Log Returns Over Time Period 2013 − 2018

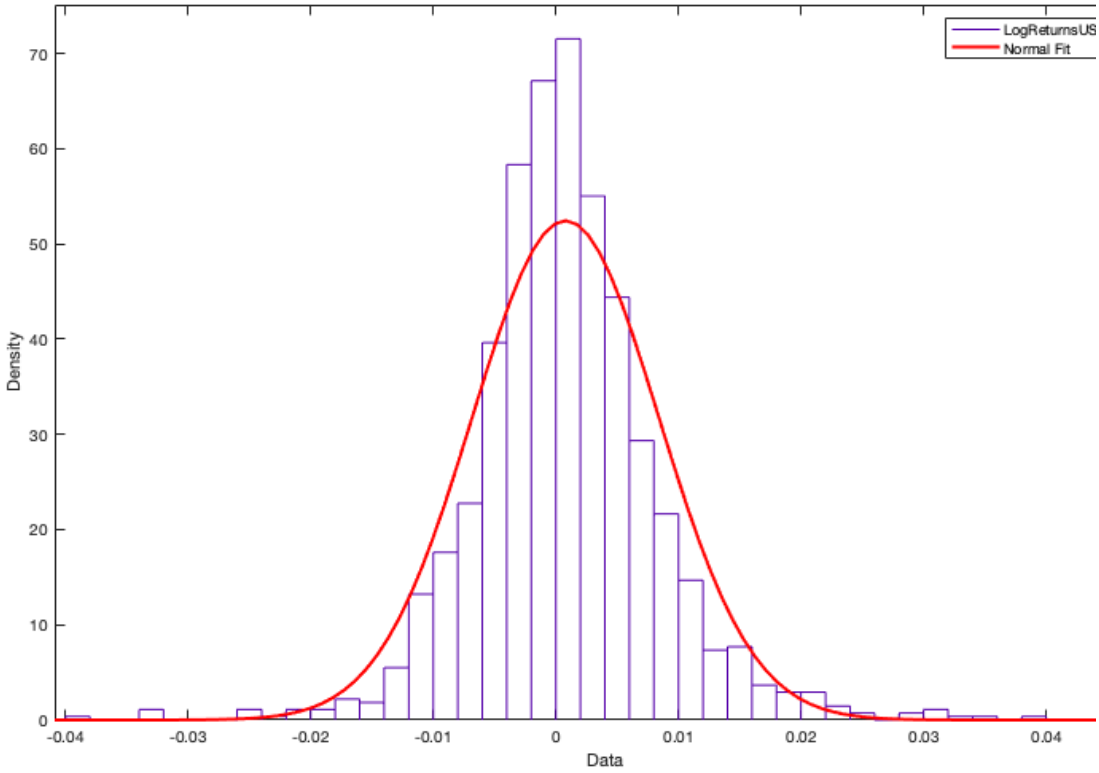


Figure 4.3: Histogram of USDTRY Daily Log Returns 2013-2018

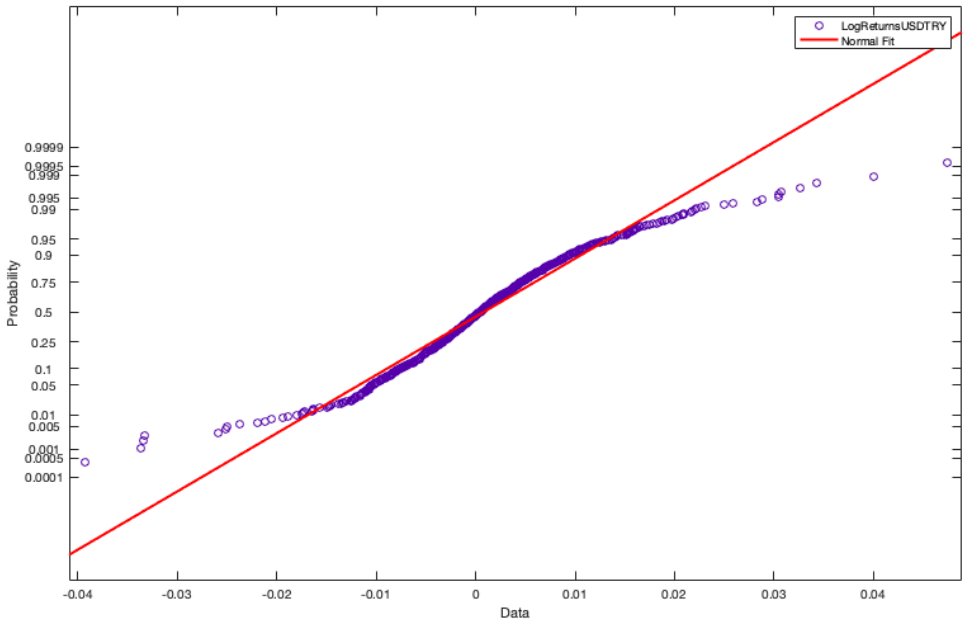


Figure 4.4: Probability Plot of Fitted USDTRY Daily Log Returns 2013-2018

## 4.2 Calibration

Here by referring calibration, we aim, searching for parameter values in order to find prices implied by the model that do not differ much from market prices. We have run calibration on daily data for each day with the least square scheme. We have used option data for tenors 1M, 3M, 6M, and 12M in the calibration procedure. We have left data with tenors 2M and 9M for out sample tests.

Mathematically expressing, for a given model and corresponding market data,

$$\hat{\theta} = \arg min \sum_{i=1}^{N} \frac{1}{\omega_i} \left( \Pi_i^{market}(\tau_i, K_i) - \Pi_i^{model}(\tau_i, K_i) \right)^2, \qquad (4.3)$$

where $N$ is the number of options $\Pi_i^{market}$ denotes corresponding market data and, $\Pi_i^{model}$ is model implied volatility. In this study we consider five option quotes and four

different time-to-maturities which led $N = 20$. We have used unit weights and liquidity weight by setting $\omega_i = 1$ and, $\omega_i = \sigma_{ask_i} - \sigma_{bid_i}$. Weighting schemes have not affected the computation time significantly.

Unit weights aim to converge absolute squared volatilities difference to zero. Intuitively, it is clear that unit weights puts more effort into correcting the options with high implied volatilities.

We have also applied a relative weighting scheme that we call "liquidity weights". We have aimed to give attention to valuable information provided by liquid quotes. The liquidity weights puts more effort into correcting the options that have narrow bid-ask spread.

We have carried the calibration process is for all 1372 days, and per day a set of parameters is found for both weighting schemes; the unit weights and the relative weights. On average, daily calibration of the unit-weights for the Heston model have taken 20 seconds whereas, liquidity-weights have taken 40 seconds on average for Heston Model on 1.6 GHz Intel Core i5 computer.

### 4.2.1 Pricing with Heston Dynamics

The calibration process becomes complex for stochastic volatility models because the calculation of a set of parameters is required, and the computational effort is much higher. The prices are computed using partial differential equation, (3.20) recalled

$$H\big(\kappa, \theta, \sigma, \rho, \lambda, r_d, r_f, v_t, S_t, K, \tau, \phi\big) = \phi\{Se^{-r_f\tau}P_+(\phi) - Ke^{-r_d\tau}P_-(\phi)\},$$

with numerical integration in MATLAB. We have employed the the built-in MATLAB function “quadgk” for numerical integration. Function “quadgk” applies adaptive quadrature using 15th and 7th order formulas for Gauss-Kronrod pair (see details in [16]).

In order to take Feller condition into account on calibration, we embed a nonlinear constraint for MATLAB ”fmincon” by limiting the linear function transformed from (3.32):

where $\varepsilon$ is taken to be $0.00000001$. Constraints for parameters are assumed by considering market practice and literature

$$\tilde{\alpha}(\sigma, \kappa, \theta) = \sigma^2 - 2\kappa\theta < \varepsilon\,, \tag{4.4}$$

where $\varepsilon$ is taken to be $0.00000001$.

Constraints for parameters are assumed by considering market practice and literature , see in [23],

$$0 < \kappa < 20\,,$$
$$0 < \theta < 1\,,$$
$$0 < \sigma < 5\,,$$
$$-1 < \rho < 1\,,$$
$$0 < v_0 < 1\,.$$

For initial guess of the start day of the calibration (11 March 2013), the initial guess for the parameters by [9] is chosen:

$$\kappa = 1.5,\ \theta = 0.05,\ \sigma = 0.66,\ \rho = 0.05,\ v_0 = 0.40.$$

For following days, the previous day's optimal values are set as parameters' initial values.

### 4.2.2 Parameter Statistics

In previous sections, we have described calibration characteristics. We have run the calibration for 1372 days in period from 11 March 2013 to 20 August 2018. We have obtained 1372 number of calibrated parameter sets $\hat{\theta}_{unit}$ and 1372 number of calibrated parameter sets $\hat{\theta}_{relative}$ for the unit weights and the relative weights respectively, Both $\hat{\theta}_{unit}$ and $\hat{\theta}_{relative}$ have been calibrated to market implied volatilities $\sigma_{market}(\Delta, \tau)$ with $(t, \Delta)$ pairs such that $\tau = 1\text{M}, 3\text{M}, 6\text{M}, \text{and } 12\text{M}$; and $\Delta = 10, 25, 50, 75$ and $90$.

In and , we have presented summary statistics of calibrated parameters for the Heston model. Note that the standard deviation of $\kappa$ is high for the Heston Model with unit weights . We have expected to see this outcome because, as seen in Figure 4.2,, mean reversion varies through time-line.

Table 4.2: Statistics of Calibrated Parameters of Heston Model with Unit Weights.

| $\hat{\theta}_{unit}$ | $\boldsymbol{\kappa}$ | $\boldsymbol{\theta}$ | $\boldsymbol{\sigma}$ | $\boldsymbol{\rho}$ | $\boldsymbol{v_0}$ |
|---|---|---|---|---|---|
| **Mean** | 4.8093 | 0.0223 | 0.4425 | 0.5988 | 0.0191 |
| **Standard Deviation** | 1.6675 | 0.0237 | 0.1259 | 0.1006 | 0.0241 |
| **Maximum** | 12.6445 | 0.5379 | 1.3614 | 0.9295 | 0.3529 |
| **Minimum** | 0.0070 | 0.0059 | 0.0865 | -0.0881 | 0.0020 |
| **Median** | 4.6133 | 0.0203 | 0.4496 | 0.5837 | 0.0143 |

Table 4.3: Statistics of Calibrated Parameters of Heston Model with Relative Weights

| $\hat{\theta}_{relative}$ | $\boldsymbol{\kappa}$ | $\boldsymbol{\theta}$ | $\boldsymbol{\sigma}$ | $\boldsymbol{\rho}$ | $\boldsymbol{v_0}$ |
|---|---|---|---|---|---|
| **Mean** | 3.1881 | 0.0256 | 0.4007 | 0.6072 | 0.0157 |
| **Standard Deviation** | 1.2015 | 0.0021 | 0.0446 | 0.0351 | 0.0073 |
| **Maximum** | 8.24356 | 0.03224 | 0.60497 | 0.69422 | 0.04356 |
| **Minimum** | 1.90034 | 0.02215 | 0.32263 | 0.50743 | 0.00582 |
| **Median** | 3.14858 | 0.02531 | 0.39635 | 0.61297 | 0.01366 |

### 4.2.3 Error Measures

In this section error measurements of the empirical research are represented. Error measurements carried on in sample and out sample outcomes.

In-sample set have been constituted by $(t, \tau_{in-sample}, \Delta)$ points such that $\tau_{in-sample} = 1\text{M}, 3\text{M}, 6\text{M}, \text{and } 12\text{M}$; and $\Delta = 10, 25, 50, 75$ and; $t$ is any business date in between 11 March 2013 and 20 August 2018. We have benefited the in-sample set during the calibration.

Out-sample set have been constituted by $(t, \tau_{out-sample}, \Delta)$ points such that $\tau_{out-sample} = 2\text{M}, 9\text{M}$; and $\Delta = 10, 25, 50, 75 \text{ and } 90$; $t$ is any business date in between 11 March 2013 and 20 August 2018. We have avoided the out-sample set while calibrating the parameters.

$\hat{\sigma}(\tau_{in-sample}, \Delta; \hat{\theta}_{relative}), \hat{\sigma}(\tau_{out-sample}, \Delta; \hat{\theta}_{relative}), \hat{\sigma}(\tau_{in-sample}, \Delta; \hat{\theta}_{unit})$ and $\hat{\sigma}(\tau_{out-sample}, \Delta; \hat{\theta}_{unit})$ are implied volatilities that calculated with the parameter sets produced by the calibration procedures, and, with the Heston's semi-closed form solution. The empirical performance was examined in terms of four measures.

The Interpolated Market Surface have been built to be used it as a benchmark on out-sample tests. Interpolation have been done to acquire volatility estimates of tenors 2-M and 9-M by formula $(4.5)$. We have achieved 1372 number of interpolated implied volatility sets: $\bar{\sigma}(\Delta, \tau_{out-sample})$ with $(\tau_{out-sample}, \Delta)$.

Following tests are, carried to compare the volatility surface generated by Heston model and, the Interpolated Market Surface. The empirical performance was examined in terms of four measures.

Mean Absolute Errors (MAE)

$$MAE = \frac{1}{N}\sum_{i=1}^{N}\left|\Pi_i^{market} - \Pi_i^{model}\right|, \tag{4.6}$$

Mean Percentage Errors (MPE)

$$MPE = \frac{1}{N}\sum_{i=1}^{N}\frac{\Pi_i^{market} - \Pi_i^{model}}{\Pi_i^{market}}, \tag{4.7}$$

Mean Absolute Percentage Errors (MAPE)

$$MAPE = \frac{1}{N}\sum_{i=1}^{N}\frac{\left|\Pi_i^{market} - \Pi_i^{model}\right|}{\Pi_i^{market}}, \tag{4.8}$$

Root Mean Squared Errors (RMSE)

$$MAE = \sqrt{\frac{1}{N}\sum_{i=1}^{N}\left(\Pi_i^{market} - \Pi_i^{model}\right)^2}, \qquad (4.9)$$

where $N$ is the number of options, $\Pi_i^{market}$ is market implied volatility and, $\Pi_i^{model}$ is model implied volatility. In this study we consider five option quotes and four different time-to-maturities which leads $N = 20$.

MAPE measure is important since it prevents offsetting by negative and positive difference. Since implied volatility is small, expressed in decimals, MAPE enables more reasonable measurements. Following tables presents measurements results.

We have interpolated for 2-M and 9-M volatilities with formula (4.10). Following tests are, carried to compare the volatility surface generated by Heston model and, the Interpolated Market Surface.

Table 4.4: In-sample Error Measures of Heston Model with Relative Weights

| $\hat{\sigma}(\tau_{in-sample}, \Delta; \hat{\theta}_{relative})$ | **MAE** | **MPE** | **MAPE** | **RMSE** |
|---|---|---|---|---|
| **Mean** | 0.0083 | 0.0108 | 0.0573 | 0.0092 |
| **Standard Deviation** | 0.0056 | 0.0605 | 0.0320 | 0.0060 |
| **Maximum** | 0.0291 | 0.1615 | 0.1615 | 0.0311 |
| **Minimum** | 0.0018 | (0.1442) | 0.0141 | 0.0024 |
| **Median** | 0.0066 | 0.0223 | 0.0518 | 0.0075 |

Table 4.5: Out-sample Error Measures of Heston Model with Relative Weights

| $\hat{\sigma}(\tau_{out-sample}, \Delta; \hat{\theta}_{relative})$ | **MAE** | **MPE** | **MAPE** | **RMSE** |
|---|---|---|---|---|
| **Mean** | 0.0220 | (0.1789) | 0.1884 | 0.0296 |
| **Standard Deviation** | 0.0023 | 0.0235 | 0.0222 | 0.0027 |
| **Maximum** | 0.0612 | 0.0087 | 0.1392 | 0.0734 |
| **Minimum** | 0.0021 | -0.0279 | 0.0136 | 0.0029 |
| **Median** | 0.0059 | -0.0029 | 0.0452 | 0.0079 |

Table 4.6: In-sample Error Measures of Heston Model with Unit Weights

| $\hat{\sigma}(\tau_{in-sample}, \Delta; \hat{\theta}_{unit})$ | **MAE** | **MPE** | **MAPE** | **RMSE** |
|---|---|---|---|---|
| **Mean** | 0.0044 | 0.0050 | 0.0179 | 0.0053 |
| **Standard Deviation** | 0.0017 | 0.0083 | 0.0097 | 0.0020 |
| **Maximum** | 0.0185 | 0.0436 | 0.0578 | 0.0221 |
| **Minimum** | 0.0002 | (0.0266) | 0.0072 | 0.0016 |
| **Median** | 0.0043 | 0.0052 | 0.0125 | 0.0053 |

Table 4.7: Out-sample Error Measures of Heston Model with Unit Weights.

| $\hat{\sigma}(\tau_{out-sample}, \Delta; \hat{\theta}_{unit})$ | **MAE** | **MPE** | **MAPE** | **RMSE** |
|---|---|---|---|---|
| **Mean** | 0.0270 | (0.2193) | 0.2376 | 0.0359 |
| **Standard Deviation** | 0.0073 | 0.0494 | 0.0518 | 0.0090 |
| **Maximum** | 0.0934 | (0.0061) | 0.3958 | 0.1156 |
| **Minimum** | 0.0015 | (0.3781) | 0.0225 | 0.0018 |
| **Median** | 0.0257 | (0.2113) | 0.2305 | 0.0346 |

Table 4.8: Out-sample Error Measures of Interpolated Market Surface

| $\overline{\sigma}(\Delta, \tau_{out-sample})$ | **MAE** | **MPE** | **MAPE** | **RMSE** |
|---|---|---|---|---|
| **Mean** | 0.0159 | 0.0398 | 0.1310 | 0.0186 |
| **Standard Deviation** | 0.0063 | 0.0125 | 0.0484 | 0.0075 |
| **Maximum** | 0.0356 | 0.0723 | 0.3108 | 0.0422 |
| **Minimum** | 0.0053 | -0.0294 | 0.0479 | 0.0062 |
| **Median** | 0.0136 | 0.0389 | 0.1207 | 0.0159 |

### 4.2.4 Market Arbitrage Score

Following statistics shows the percentage of model implied volatilities that are lie in between market bid-ask implied volatilities. This measure examines models for arbitrage opportunity. If a price estimate of a model fails to fall in between bid-ask prices it will generate arbitrage opportunity for counterparts.

In Figure 4.5 and Figure 4.6 vertical axis shows the percentage of model implied volatilities that are in between market bid-ask implied volatilities at the same date for the delta in horizontal axis.

In Figure 4.5 in-sample results of the Heston model with the unit weights and the relative weights have been presented. The bid-ask range for 25-delta and 75-delta is not demanding, for both Heston model with the unit weights and the relative weights can keep their estimates in the market bid-ask region. The Heston model with the unit weights have been more successful to fit bid-ask range for 90-delta; The Heston model with the relative weights have been more successful to fit bid-ask range for 10-delta, but with no significant difference. 50-delta, (at-the-money) is the point that given most

attention by the market players. Not surprising that at-the-money is the most liquidly trade quote. The Heston model with the relative weights have been more successful to fit the bid-ask range for 50-delta but, could not manage to be more than 90%.

In Figure 4.6 out-sample results of the Heston model with the unit weights and the relative weights and Interpolated-Market-Surface have been presented. Interpolated-Market-Surface will be used as a benchmark for traders' tolerance. Again, the bid-ask range for 25-delta and 75-delta is not demanding, for both Heston model with the unit weights and the relative weights can keep their estimates in the market bid-ask region and they are significantly better than the benchmark. The Heston model with the unit weights have been more successful to fit bid-ask range for 90-delta; The Heston model with the relative weights have been more successful to fit bid-ask range for 10-delta, but with no significant difference to the other and to the benchmark as well. 50-delta, (at-the-money) is the point that given most attention by the market players. The Heston model with the relative weights have been the most successful to fit the bid-ask range for 50-delta, the most important point, with a significant difference, even in the out-sample set.

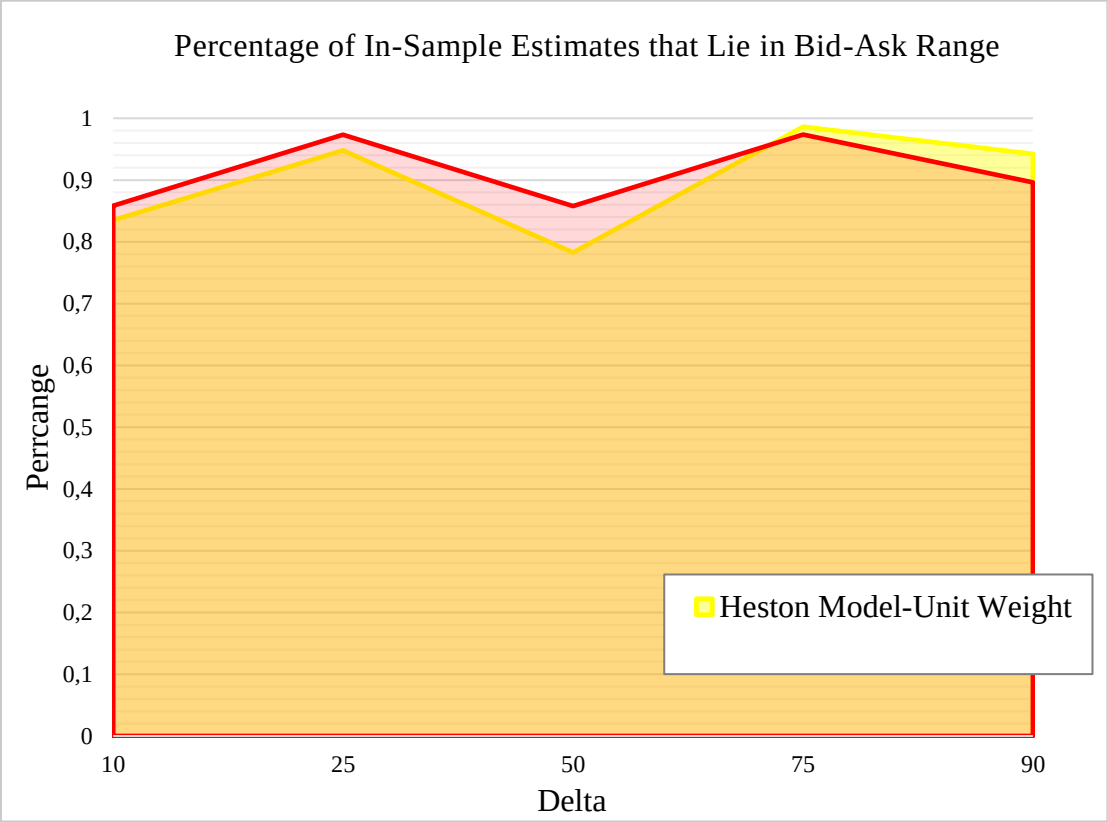


Figure 4.5: In-sample Ability to Fall in Bid-Ask Spread

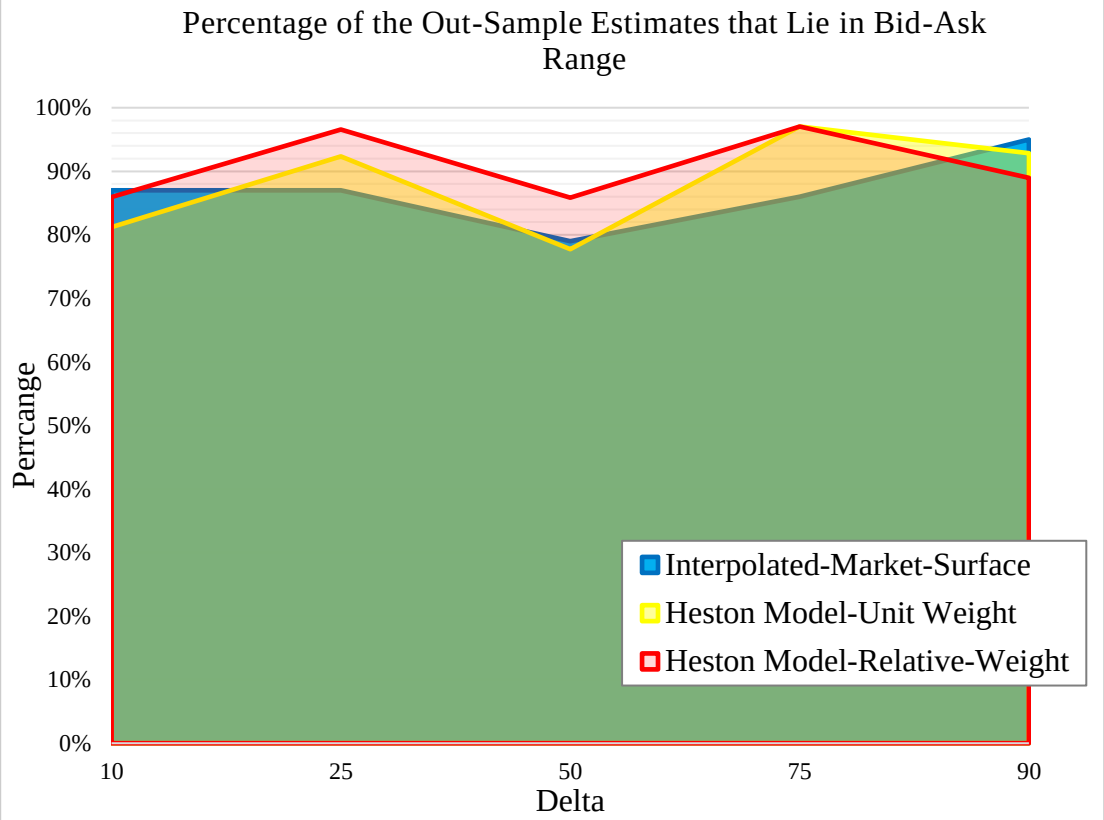


Figure 4.6: Out-sample Ability to Fall in Bid-Ask Spread

### 4.2.5 Calibration Performance by Term

In this section volatility smiles comparison of The Heston model with the unit weights and the relative weights and Interpolated-Market-Surface by terms are represented for 1-month, 3-month, 6 month and 1-year tenors. We emphasize that Heston model is able to follow market implied volatilities. The Heston model with the relative weights follows closer the market especially for ATM node.

We have also presented the volatility smiles comparison of The Heston model with the unit weights and the relative weights and Interpolated-Market-Surface by terms for 2-month tenor and, 9-month tenor. The Heston model is not differing much to follow market dynamics compared to the benchmark performance to follow model dynamics.

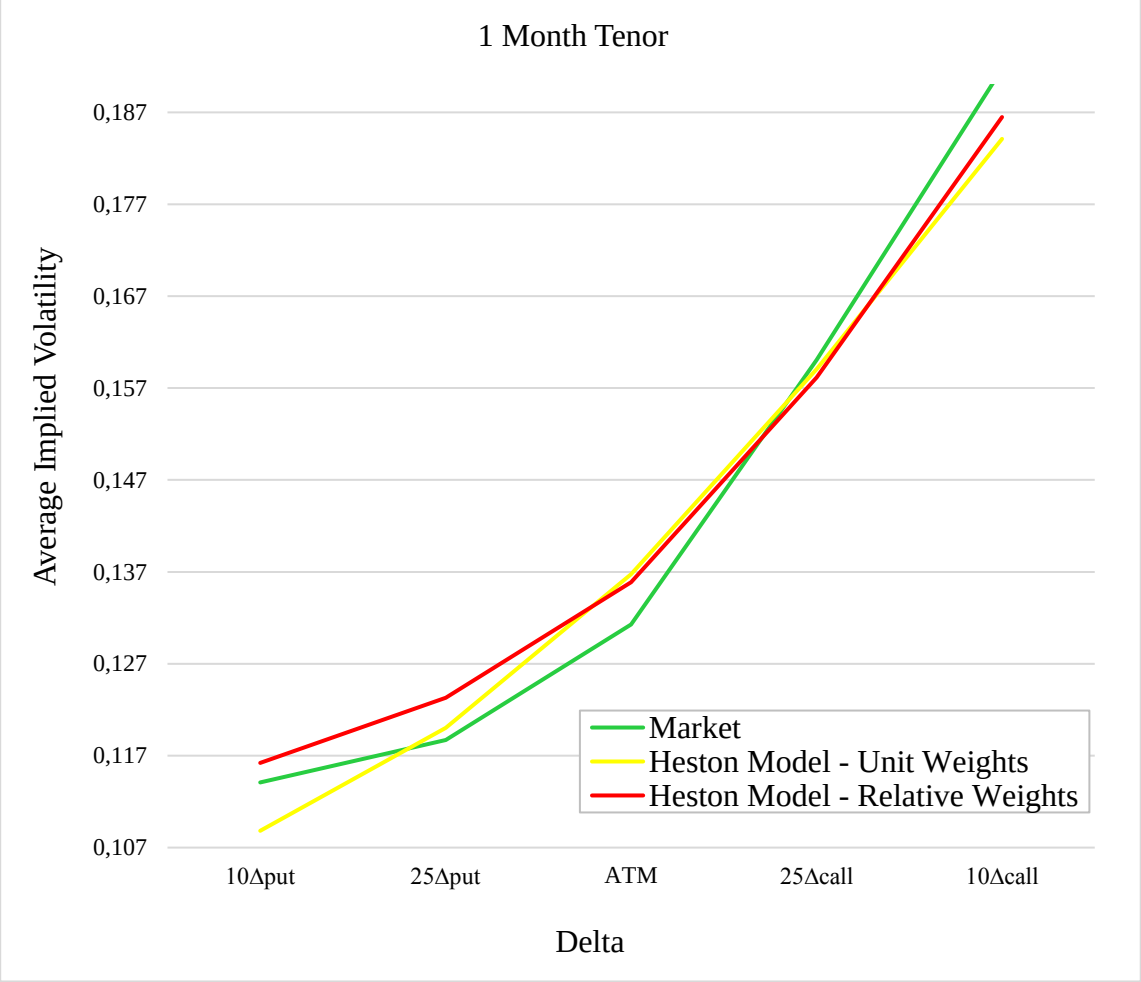


Figure 4.7: Implied Volatility Comparison for 1 Month Tenor. Each Volatility Smile Represents the Average Implied Volatilities for period between 11 March 2013 and 20 August 2018.

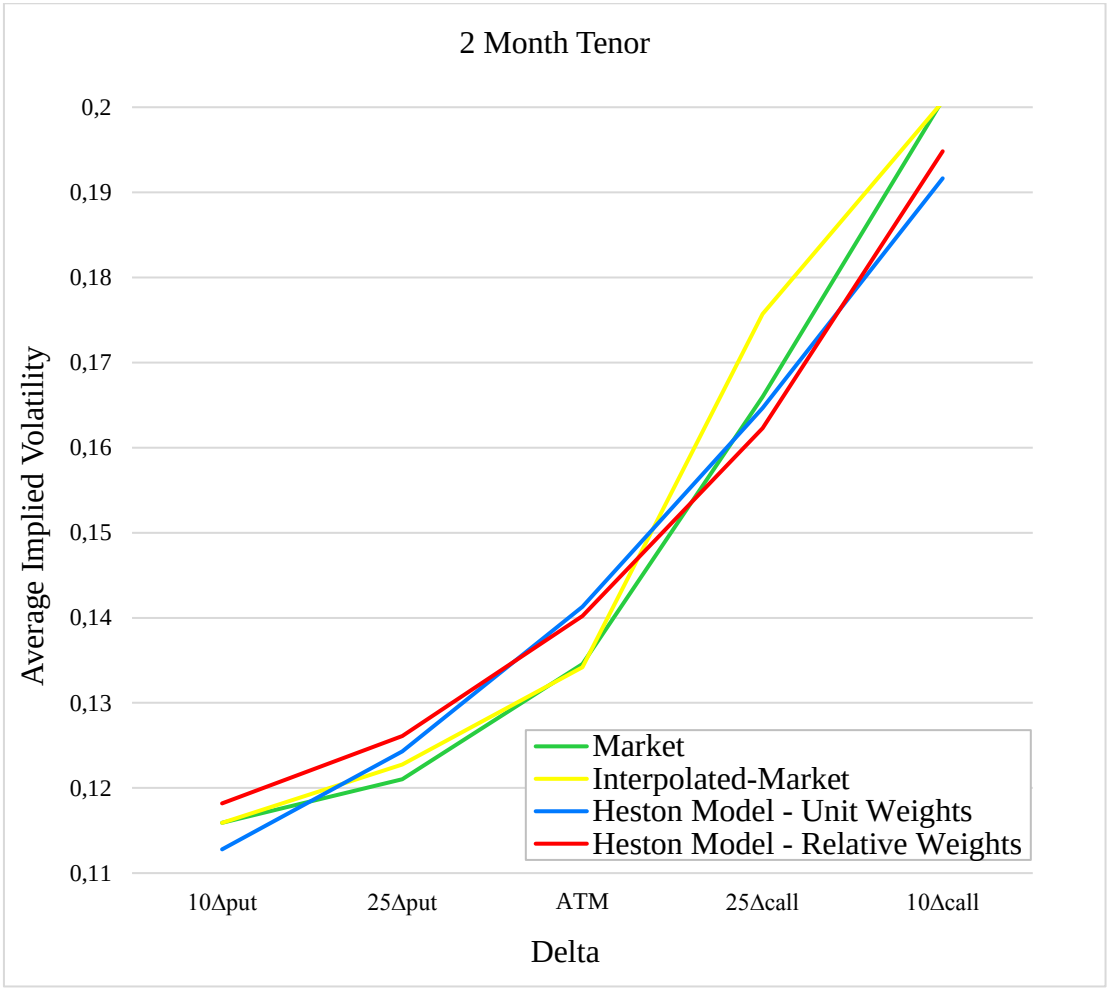


Figure 4.8: Implied Volatility Comparison for 2 Month Tenor. Each Volatility Smile Represents the Average Implied Volatilities for period between 11 March 2013 and 20 August 2018.

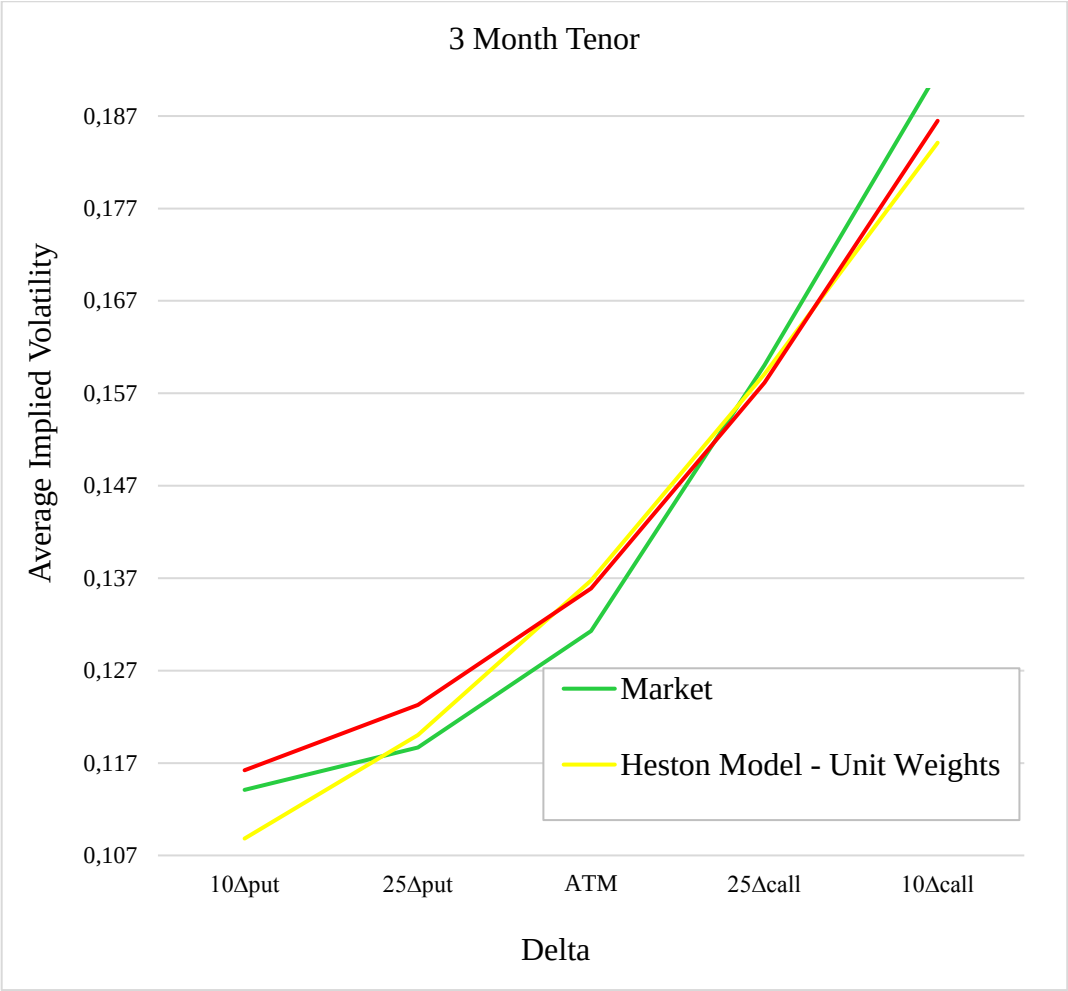


Figure 4.9: Implied Volatility Comparison for 3 Month Tenor. Each Volatility Smile Represents the Average Implied Volatilities for period between 11 March 2013 and 20 August 2018.

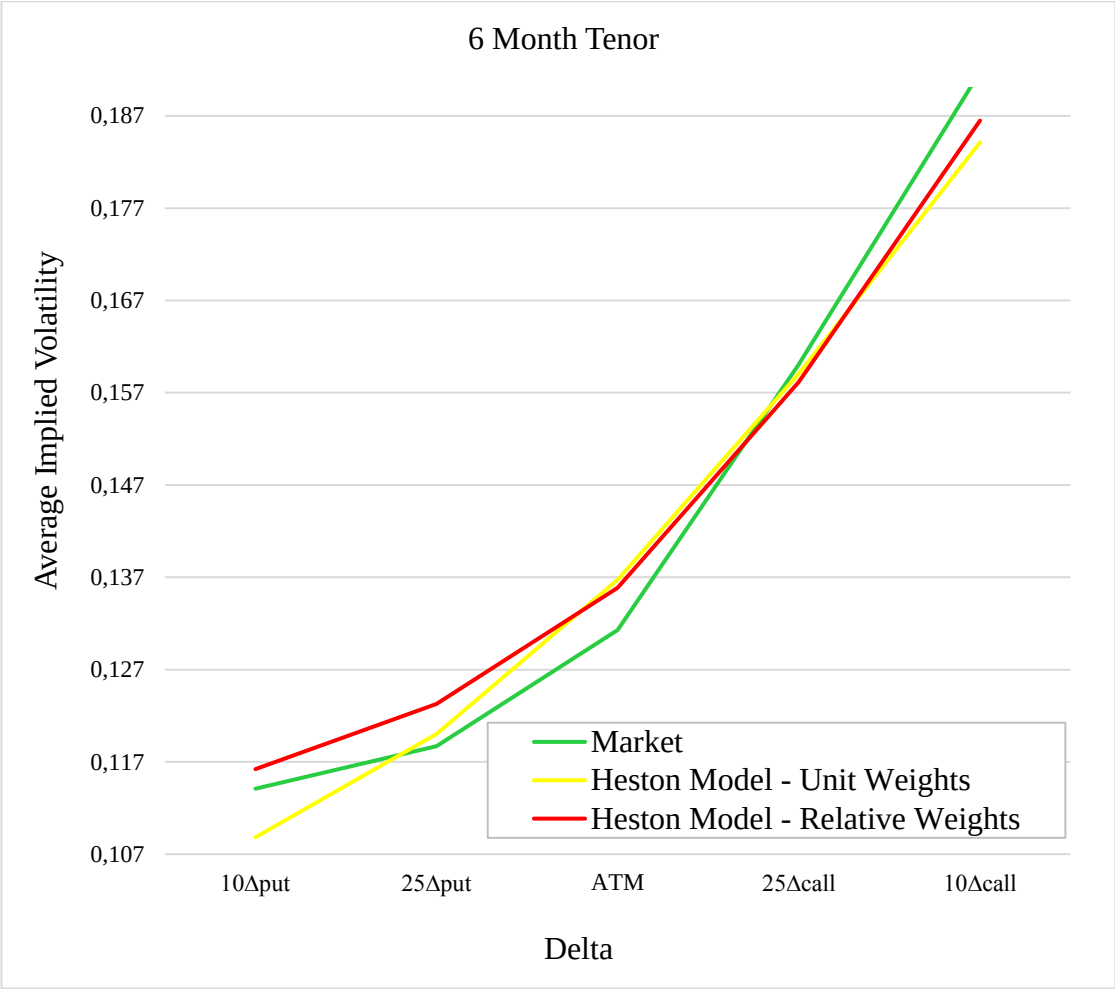


Figure 4.10: Implied Volatility Comparison for 6 Month Tenor. Each Volatility Smile Represents the Average Implied Volatilities for period between 11 March 2013 and 20 August 2018.

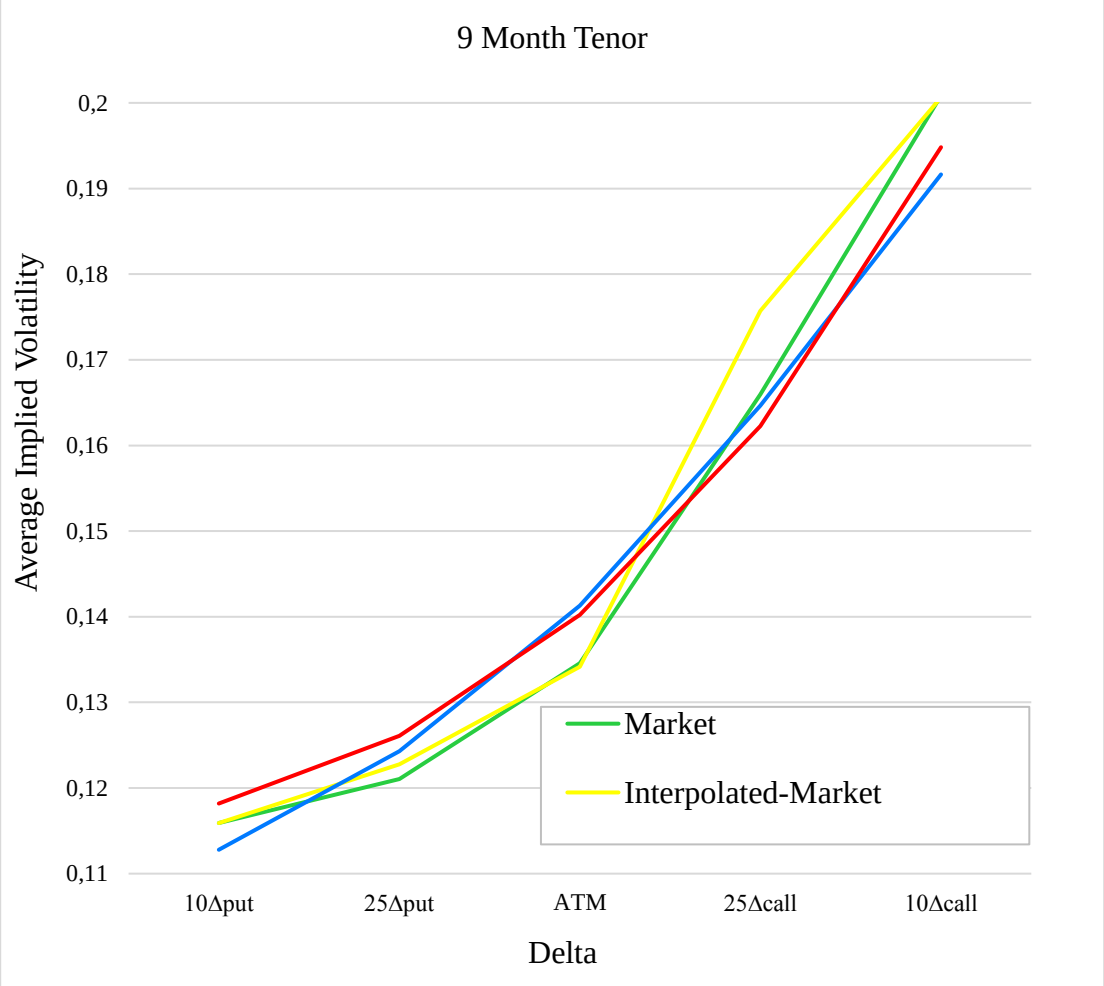


Figure 4.11: Implied Volatility Comparison for 9 Month Tenor. Each Volatility Smile Represents the Average Implied Volatilities for period between 11 March 2013 and 20 August 2018.

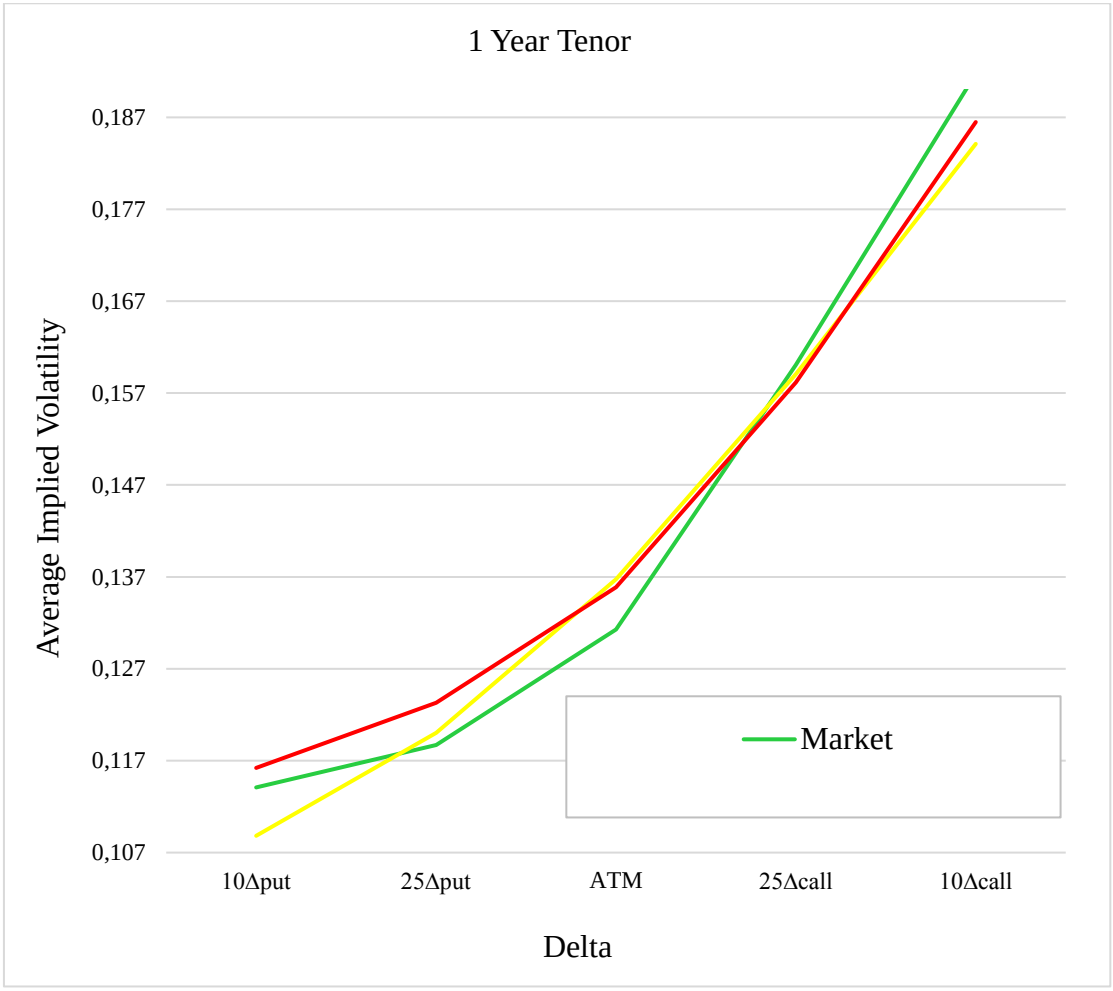


Figure 4.12: Implied Volatility Comparison for 1 Year Tenor. Each Volatility Smile Represents the Average Implied Volatilities for period between 11 March 2013 and 20 August 2018.

Surface of Average Implied Volatilities estimated by The Heston model with the unit weights and the relative weights and Interpolated-Market-Surface is shown in following figures.

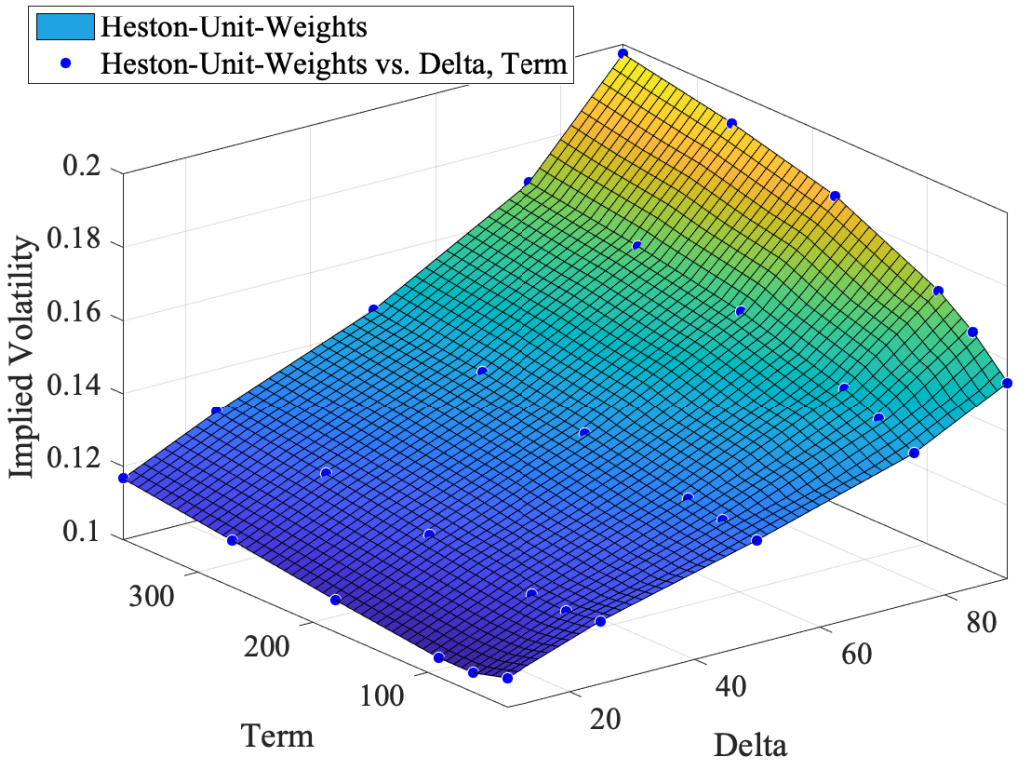


Figure 4.13: Surface of Average Implied Volatilities estimated by Heston Model with Unit Weights.

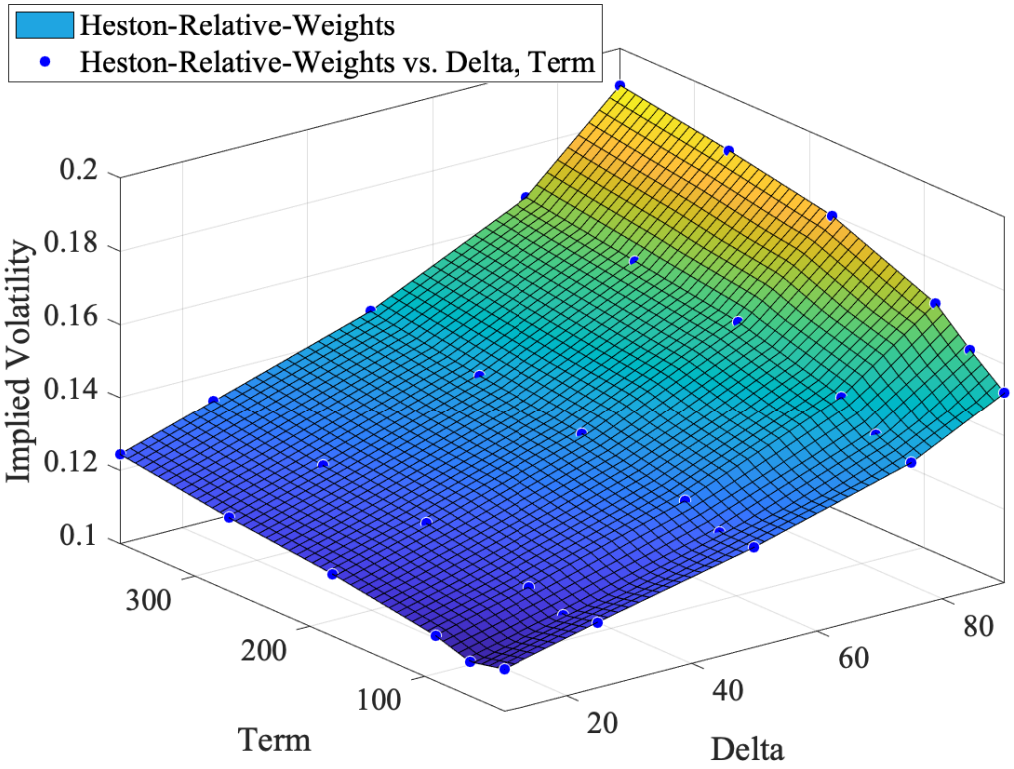


Figure 4.14: Surface of Average Implied Volatilities estimated by Heston Model with Relative Weights.

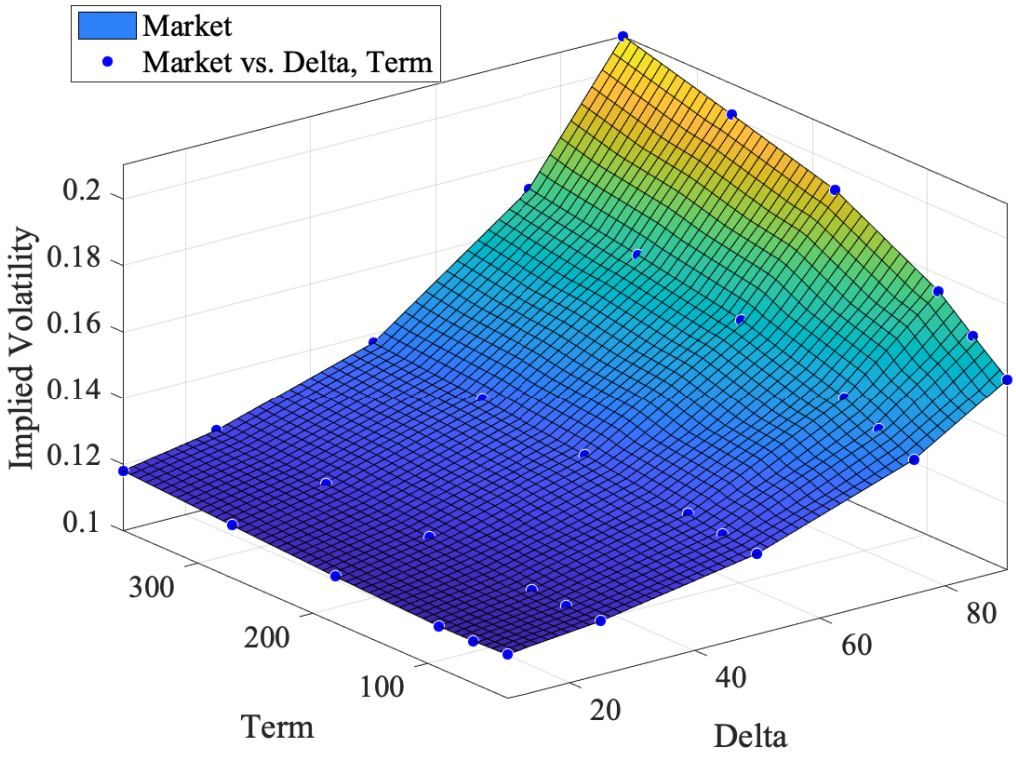


Figure 4.15: Surface of Average Volatilities implied by the Market.

# CHAPTER 5

# CONCLUSION

In this thesis, we aimed to investigate time contingent behavior of risk factor USDTRY. To estimate the behavior, we have benefited option pricing models Black-Scholes with market interpolated volatility surface and Heston model with two different weighting schemes.

Since risk-neutral valuation requires, we have designed another process to estimate the risk-free rates for both USD and TRY currency. We have governed OIS discounting framework for risk-free rate estimate. To best of our knowledge, this is the first study that benefits OIS discounting to estimate a risk-free rate for TRY nominated instruments.

We have conducted in-sample and out-sample tests to measure the estimation power of the models. We have also investigated the model performance by varying tenors. We have developed a method to measure the models if they are precise enough to generate implied volatilities in the observed bid-ask range of the market.

In context of the measurements, the Heston model, especially with liquidity weights, has managed to follow the market dynamics and produce similar error

performance per the benchmark, the Adjusted Black-Scholes model. Calculation costs required by the Heston model have not differed from the Black-Scholes' computation costs, significantly, since the Heston model provides a semi-closed form option valuation. Moreover, the Heston model can provide risk-neutral or arbitrage-free pricing as an advantage and does not breach the tolerance that traders' have been welcome already.

We have observed that incorporating the liquidity weights significantly have improved the Heston model performance. Future work would be to use the bid-ask prices during the calibration process as a boundary condition. Then, we could expect a higher percentage for implied volatility estimates that have not breached the bid-ask limits. On the other hand, the effects of the bid-ask boundary conditions on calibration time and parameter development should be monitored.

## REFERENCES


[1] H. Albrecher, P. Mayer, W. Schoutens, and J. Tistaert, "The little Heston trap.," *Wilmott*. vol. 6, pp. 83–92, 2007.

[2] Bank for International Settlements, *Triennial Central Bank Survey - Foreign exchange turnover in April 2016.*, 2016.

[3] T. Björk, *Arbitrage Theory in Continuous Time*. *Oxford University Press*, 2005.

[4] F. Black and M. Scholes, "The Pricing of Options and Corporate Liabilities.," *Journal of Political Economy*. vol. 81, pp. 637–654, 1973.

[5] B. Blanco, "Capturing the volatility smile: parametric volatility models versus stochastic volatility models.," *Public and Municipal Finance*. vol. 5, no. 4, pp. 15–22, 2016.

[6] I.J. Clark, *Foreign Exchange Option Pricing: A Practitioner's Guide*. *Wiley*, 2011.

[7] Z. Dadachanji, *FX Barrier Options: A Comprehensive Guide for Industry Quants*. *Palgrave Macmillan*, 2015.

[8] B. (Bloomberg) Dupire, "Pricing with a Smile.," *Risk*. vol. 7, pp. 1–10, 2004.

[9] C. Eratman, "Two Essays in Modeling and Analysis of Exchange Rate," (2011).

[10] S.L. Heston, "A Closed-Form Solution for Options with Stochastic Volatility with Applications to Bond and Currency Options.," *Review of Financial Studies*. vol. 6, no. 2, pp. 327–343, 1993.

[11] J.C. Hull, A.D. White, J.C. Hull, and A. White, "The Pricing of Options on Assets with Stochastic Volatilities.," *Journal of Finance*. vol. 42, no. 2, pp. 281–300, 1987.

[12] J. Hull and A. White, "LIBOR vs. OIS.," *Journal Of Investment Management*.

vol. 11, no. 3, pp. 14–27, 2013.

[13] A. Janek, T. Kluge, R. Weron, and U. Wystup, “FX smile in the Heston model.,” In: *Statistical Tools for Finance and Insurance*. pp. 133–162. *Springer Berlin Heidelberg* (2011).

[14] D. Kucuksarac, A. Kazdal, I.E. Guney, İ.E. Güney, A. Kazdal, and D. Küçüksaraç, *Estimation of Currency Swap Yield Curve*. *Research and Monetary Policy Department, Central Bank of the Republic of Turkey*, 2018.

[15] A.M. Malz, “A Simple and Reliable Way to Compute Option-Based Risk-Neutral Distributions.,” *SSRN Electronic Journal*. p. 2014.

[16] MathWorks, “Numerically evaluate integral, adaptive Gauss-Kronrod quadrature - MATLAB quadgk,” https://www.mathworks.com/help/matlab/ref/quadgk.html.

[17] R.C. Merton, “Theory of rational option pricing.,” *Bell J Econ Manage Sci*. vol. 4, no. 1, pp. 229–288, 1973.

[18] A. Persson, “Calibration of FX options and pricing of barrier options,” (2013).

[19] D. Reiswich and W. Uwe, “FX Volatility Smile Construction.,” *Wilmott*. vol. 2012, no. 60, pp. 58–69, 2012.

[20] M. Rubinstein, “Implied Binomial Trees.,” *The Journal of Finance*. vol. 49, no. 3, pp. 771–818, 1994.

[21] L.O. Scott, “Option Pricing when the Variance Changes Randomly: Theory, Estimation, and an Application.,” *The Journal of Financial and Quantitative Analysis*. vol. 22, no. 4, p. 419, 1987.

[22] J.B. Wiggins, “Option values under stochastic volatility: Theory and empirical estimates.,” *Journal of Financial Economics*. vol. 19, no. 2, pp. 351–372, 1987.

[23] U. Wystup, *FX Options and Structured Products*. *John Wiley & Sons, Ltd*, Chichester, UK, 2017.